Received: 19 April 2023 | Revised: 9 October 2023 | Accepted: 6 November 2023

DOI: 10.1002/hyp.15034

RESEARCH ARTICLE

WILEY

An appraisal of the local-scale spatio-temporal variations of drought based on the integrated GRACE/GRACE-FO observations and fine-resolution FLDAS model

Behnam Khorrami[1] | Shoaib Ali[2] | Orhan Gündüz[3]

[1]Department of GIS, The Graduate School of Natural and Applied Sciences, Dokuz Eylul University, Izmir, Turkey

[2]Department of Earth and Space Sciences, Southern University of Science and Technology, Shenzhen, China

[3]Department of Environmental Engineering, Izmir Institute of Technology, Izmir, Turkey

Correspondence
Behnam Khorrami, Department of GIS, The Graduate School of Natural and Applied Sciences, Dokuz Eylul University, Izmir, Turkey.
Email: behnam.khorrami@ogr.deu.edu.tr

Abstract

The gravity recovery and climate experiment (GRACE) observations have so far been utilized to detect and trace the variations of hydrological extremes worldwide. However, applying the coarse resolution GRACE estimates for local-scale analysis remains a big challenge. In this study, a new version of the fine resolution (1 km) Famine early warning systems network Land Data Assimilation System (FLDAS) model data was integrated into a machine learning model along with the GRACE data to evaluate the subbasin-scale variations of water storage, and drought. With a correlation of 0.99 and a root mean square error (RMSE) of 3.93 mm of its results, the downscaling model turned out to be very successful in modelling the finer resolution variations of TWSA. The water storage deficit (WSD) and Water Storage Deficit Index (WSDI) were used to determine the episodes and severity of drought events. Accordingly, two severe droughts (January 2008 to March 2009 and September 2019 to December 2020) were discerned in the Kizilirmak Basin (KB) located in Central Türkiye. The characterization of droughts was evaluated based on WSDI, scPDSI, and model-based drought indices of the soil moisture storage percentile (SMSP) and groundwater storage percentile (GWSP). The results indicated discrepancies in the drought classes based on different indices. However, the WSDI turned out to be more correlated with GWSP, suggesting its high ability to monitor groundwater droughts as well.

KEYWORDS
downscaling, drought, FLDAS, GRACE, Kizilirmak basin, random forest

1 | INTRODUCTION

Drought is defined as prolonged dry conditions manifested in terms of water deficits. As a dynamic event, it is one of the most catastrophic environmental phenomena happening with a high frequency and prolonged duration. It has severe consequences for agriculture, ecological integrity, and socio-economic progress (Kumar, AnandRaj, et al., 2021). The rising temperatures, as a result of the climate crisis, have increased global evapotranspiration amounts and have altered the spatio-temporal distribution of the hydrological cycle components, in particular, precipitation (Zhou et al., 2021). These alterations have resulted in variations in extreme drought events in numerous spatial

and temporal domains (Trenberth et al., 2014). Different drought events can occur at different severity levels, which may demonstrate variations spatially, thus their side effects may depend on the vulnerability of affected sectors (Kisi et al., 2019). Therefore, knowledge of precise variations in the spatio-temporal characteristics of drought is crucial, especially in regions where water storage is linked to regional security (Famiglietti, 2014) through which effective mitigation and adaptation strategies can be followed to reduce the vulnerability of human societies (Nischitha et al., 2014). The importance of drought assessment at spatial and temporal domains was underscored by several researchers over different case study areas such as Portugal (Santos et al., 2010), China (Xu et al., 2015), Inner Mongolia in China (An et al., 2020), Iran (Noorisameleh et al., 2021). The issue is also of utmost importance in the arid and semi-arid areas of the world (Richey et al., 2015). The exact identification of drought, however, is restrained by our inability to directly observe changes in water storage. Droughts are traditionally analysed through in situ observations of hydrometeorological parameters. This orthodox monitoring approach is limited by ground data availability such as the heterogeneous distribution of the stations at a spatial scale and the scarcity of continuous observations in time (Khorrami & Gunduz, 2021a). To date, several standardized indices have been developed to investigate the precise spatio-temporal characteristics of droughts, among which the Palmer Drought Severity Index (PDSI), Standardized Precipitation Index (SPI), and Standardized Precipitation-Evapotranspiration Index (SPEI) are the most widely used ones (Mckee et al., 1993; Palmer, 1965; Vicente-Serrano et al., 2010). However, these indices are associated with certain drawbacks that restrict their effectiveness in the accurate reproduction of drought conditions (Sehgal et al., 2017).

Due to the recent achievements in the field of remote sensing, particularly with the advent of the Gravity Recovery And Climate Experiment (GRACE), uninterrupted, precise, and economic assessment and evaluation of water storage is now possible from regional to global scales. The GRACE offers the estimates of Terrestrial Water Storage Anomalies (TWSA), which include different components of the hydrological cycle such as Groundwater Storage Anomalies (GWSA), Surface Water Storage Anomalies (SWSA), Soil Moisture Storage Anomalies (SMSA), and Snow Water Equivalent Anomalies (SWEA) (Equation 1) that is stored above and beneath the land surface (Ali et al., 2021; Ali, Liu, et al., 2022; Ali, Wang, et al., 2022; Arshad et al., 2022; Khorrami et al., 2022; Khorrami & Gündüz, 2023).

$$\mathrm{TWSA} = \mathrm{SMSA} + \mathrm{SWEA} + \mathrm{SWSA} + \mathrm{GWSA}. \quad (1)$$

The GRACE observations have so far been applied for the large-scale assessment of water storage, groundwater storage, and drought (e.g., Abhishek, 2022; Ali et al., 2023; Guo et al., 2021; Khorrami et al., 2022; Khorrami, Ali, Sahin, & Gunduz, 2023; Khorrami & Gunduz, 2021a; Khorrami & Gündüz, 2022; Li et al., 2019; Liu, Pei, & Shen, 2022; Tariq et al., 2023; Wang et al., 2020; Wang et al., 2022; Zhao et al., 2022). The GRACE-based drought indicators such as total storage deficit index (TSDI) (Yirdaw et al., 2008), water storage deficit (WSD) (Thomas et al., 2014), GRACE-based hydrological drought index (GHDI) (Yi & Wen, 2016), GRACE-drought severity index (GDSI) (Zhao, Velicogna, & Kimball, 2017), Water Storage Deficit Index (WSDI) (Sinha et al., 2017), Modified Total Storage Deficit Index (MTSDI) (Hosseini-Moghari et al, 2019), combined climatologic deviation index (CCDI) (Sinha et al., 2019), and enhanced water storage deficit index (EWSDI) (Khorrami & Gunduz, 2021a) have been developed and used worldwide. However, the challenging point is that the resulting indicators have the same spatial and temporal (monthly) characteristics as those of GRACE and GRACE-FO data, making them unsuitable for operational drought monitoring on regional to local scales (Li & Rodell, 2021). Although the GRACE data are more suitable for large-scale hydrological applications due to their coarse resolution, recent developments in downscaling techniques make GRACE data suitable to assess the local scale variations in water storage in some studies (e.g., Ali et al., 2021; Ali, Liu, et al., 2022; Arshad et al., 2022; Gerdener et al., 2020; Gyawali et al., 2022; Jyolsna et al., 2021; Khorrami et al., 2021; Khorrami, Pirasteh, Ali, et al., 2023; Seo & Lee, 2019; Yin et al., 2022). However, the majority of the downscaling practices have so far focused on medium-resolution (25 km × 25 km) analysis because of the limitations of fine-resolution hydrological inputs. To our best knowledge, there are only two research items implemented so far to evaluate 1 km variations of terrestrial and groundwater storage based on some fine-resolution hydrological parameters where Zhou et al. (2021) applied high-resolution vegetation index and temperature and Zhang et al. (2021) used high-resolution variables such as NDVI, soil parameters, temperature, population and Digital Elevation Model (DEM) in their studies.

As one of the world's climatic variability hotspots with a dominating arid to semi-arid climate, Türkiye is overly susceptible to drought risk, in which progressive and dramatic drier seasons at higher levels of global warming seem to be ineluctable (Pekpostalci et al., 2023). The climate change impacts accompanied by the geographic characteristics of the region have rendered the majority of the country, particularly the central, southern, and southeastern regions, prone to water scarcity (Kurnaz, 2014) where agriculture is the main economic sector (Komuscu, 1999). Drought incidents may spawn grave socio-economic side-effects in the country. For example, according to Dellal and McCarl (2010), up to 15% of the national agricultural production of Türkiye was negatively affected by the extreme drought in 2007, culminating in the loss of welfare of the population. Although drought events over Türkiye have been explored by a myriad of studies (e.g., Khorrami & Gunduz, 2021a; Khorrami & Gündüz, 2022; Kurnaz, 2014; Pekpostalci et al., 2023), no previous study have implemented a downscaled GRACE data integrated assessment procedure. Therefore, the main novelty of the current study is to evaluate the spatiotemporal patterns of drought using downscaled GRACE estimates. In this premise, a model-based Random Forest integrated methodology is proposed to downscale the GRACE/GRACE-FO data to the fine spatial resolution of 1 km × 1 km resolution. Although the FLDAS outputs have recently been utilized for the downscaling of the GRACE data (Khorrami, Ali, & Gunduz, 2023; Khorrami & Gündüz, 2023), their target resolution was 10 km × 10 km. In this study, the authors go one step further in generating high-resolution

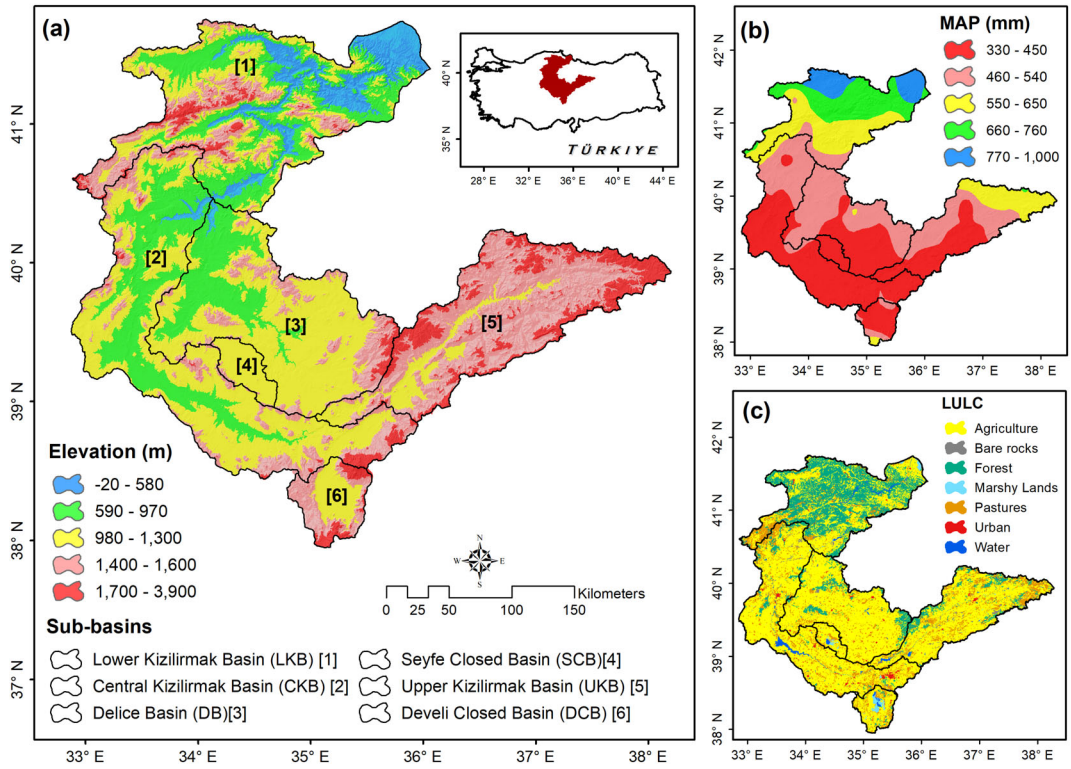

FIGURE 1 The geographic location of Kizilirmak Basin (KB) in Central Türkiye (a); Mean Annual Precipitation (MAP) (b), and Land Use/Cover (LULC) (c) of the KB.

(1km × 1km) TWSA data by integrating the newly released version of the Famine early warning systems network Land Data Assimilation System (FLDAS) model. The authors hypothesize that the fine resolution TWSA from GRACE-FLDAS integrated approach would yield acceptable results for the assessment of the subbasin-scale variations of water storage and drought incidents on a spatial and temporal domain. Within the scope of the current study, the authors aim (1) to downscale the GRACE/GRACE-FO observations based on the fine resolution FLDAS model outputs; (2) to investigate the subbasin-wise fluctuations of TWSA over subbasins of Kizilirmak Basin (KB); (3) to evaluate the subbasin-wise variations of drought; (4) to analyse the spatio-temporal characteristics of drought incidents based on the 1 km Water Storage Deficit Index (WSDI); and (5) to validate the results against global drought indices.

2 | METHODOLOGY

2.1 | Site description

As one of the most significant hydrological units of Türkiye, The Kizilirmak Basin (KB) is positioned in eastern central Anatolia. The KB is the second largest basin of the country with a drainage area of 82 221 km^2 where about 4 million people reside in 18 provinces (FMP, 2019). The basin receives an estimated precipitation of 455 mm per annum with an air temperature of 13.7°C (Hinis & Geyikli, 2023). There are six sub-basins in the basin, including the Upper Kizilirmak Basin (UKB), Lower Kizilirmak Basin (LKB), Central Kizilirmak Basin (CKB), Delice Basin (DB), Seyfe Closed Basin (SCB), and Develi Closed Basin (DCB) (Figure 1). Although the generic climate of the basin is of central Anatolian continental type (Ercan & Yüce, 2017), the microclimate of sub-basins varies according to local terrain and morphological differences (FMP, 2019). Essentially, the inner parts of the KB belong to the arid to semiarid climate type, while the coastal regions near the Black Sea have humid to semihumid conditions. The basin experienced widespread droughts between 1960 and 2017 (Akturk et al., 2022). The concomitant effects of drought vary concerning the spatial location of the incidents in the basin and have serious consequences for agricultural productivity, ecosystem integrity, and the socioeconomic well-being of the KB (DMP, 2019). Therefore, monitoring the incidents and taking effective measures in the basin are of utmost importance.

2.2 | Data sets used

As discussed below, this study used a variety of remote sensing and model data, the characteristics of which are listed in Table S1. Moreover, the methodological flow of the analysis is portrayed in Figure S1.

2.2.1 | GRACE/GRACE-FO observations

GRACEThe is a pioneering remote sensing mission with two identical satellites onboard to sense the variations in the Earth's gravitational pull (Tapley et al., 2004). The GRACE and GRACE-FO satellites both have a similar satellite orbit configuration. However, the latter benefits from an optimized system design where a Laser Ranging Interferometer (LRI) is used for testing purposes for upcoming remote sensing gravimetry projects (Chen et al., 2022). To date, the GRACE project has been a very promising space mission in rendering services to the end-users with its precious observations of terrestrial water storage anomalies (TWSA) at spatial resolutions ranging from 100 to 25 km, depending on the processing level (Khorrami et al., 2022). The gravity signals of the CSR (Center for Space Research) mascon solutions manifest higher spatial resolution (25 km) than those from other GRACE mascon solutions (Save et al., 2016). The TWSA estimates were extracted for the study area from the GRACE-CSR mascon data set accessed from http://www2.csr.utexas.edu/grace/RL06_mascons.html.

2.2.2 | FLDAS model

The FLDAS is a multifaceted modelling project (McNally et al., 2017) through which a broad range of input data from in situ observations to remotely sensed data such as precipitation, temperature, humidity, radiation, and wind is assimilated into a global model to generate intended hydro-meteorological parameters such as soil moisture, evapotranspiration, and runoff (Loeser et al., 2020; McNally et al., 2017). This model utilizes two land surface models (LSMs) in its simulation process: the Variable Infiltration Capacity (VIC) model and the Noah model (McNally et al., 2017), the spatial resolution of which ranges from 25 to 1 km. In this study, the fine resolution (1 km) of the downscaling training data sets was extracted from the newest version of the FLDAS-Noah model which covers the Central Asia region. The FLDAS model outputs can be accessed at https://disc.gsfc.nasa.gov/datasets?keywords=FLDAS.

2.2.3 | GLDAS model

The Global Land Data Assimilation System (GLDAS) is a hydrological model, akin to the FLDAS, by which different parameters are simulated through the integrated data assimilation process. The GLDAS mission uses five LSMs, such as the community land model (CLM), Variable Infiltration Capacity (VIC) model, Noah model, Mosaic model, and Catchment Land Surface Model (CLSM) (Hu et al., 2019). VIC, Mosaic, and CLSM have a spatial resolution of 100 km, while the Noah and CLSM models produce data at a resolution of 25 km. NASA has released a new version of the GRACE-CLSM assimilated drought indicators on a global scale. The soil moisture and groundwater storage situation is estimated using a complex numerical model of water and energy fluxes to come up with the soil moisture and groundwater drought indicators to evaluate the wet and dry conditions (Houborg et al., 2012). The probability of a drought incident is given as percentiles indicating wet or dry conditions (Table S2). The soil moisture and groundwater drought indices from the GLDAS-CLSM model are accessible at https://disc.gsfc.nasa.gov/datasets/GRACEDADM_CLSM025GL_7D_3.0/summary?keywords=GRACE-DA.

2.2.4 | Climate hazards group infrared precipitation with station data

The climate hazards group infrared precipitation with station data (CHIRPS) is a global precipitation data set that offers estimates of precipitation at daily and monthly scales. Much appreciated for its accurate estimates, the CHIRPS is utilized as a surrogate for precipitation perceptions, particularly over locales with data availability issues (Paca et al., 2020). The CHIRPS data set is available at http://chg.geog.ucsb.edu/data/chirps/.

2.2.5 | Self-calibrating palmer drought severity index

The self-calibrating palmer drought severity index (scPDSI) is an improved version of the palmer drought severity index (PDSI). The PDSI is based on the water balance approach and assimilates the historical data of precipitation and temperature into soil characteristics to infer drought conditions (Briffa et al., 2009). Wells et al. (2004) developed the scPDSI to compensate for the weakness of the PDSI for applications over regions with climatic diversity. For details on the calculation of the index can be found in refer to Wells et al. (2004). The grid-based scPDSI data with a spatial resolution of 50 km and on a monthly time scale were received from https://crudata.uea.ac.uk/cru/data/drought/. Table S3 gives the corresponding drought classes.

2.2.6 | Soil moisture and groundwater drought indices

Soil moisture storage percentile (SMSP), and groundwater storage percentile (GWSP) are model-based drought metrics generated through sophisticated data assimilation techniques. These drought indicators express wet or dry conditions as a percentile, indicating the probability of occurrence within the period of record from 1948 to 2014. NASA provides the global-scale gridded data simulated under the GLDAS-CLSM model, which can be accessed via https://disc.gsfc.nasa.gov/datasets/GRACEDADM_CLSM025GL_7D_3.0/summary?keywords=GRACE-DA.

2.3 | Methods

2.3.1 | Random forest machine learning

Random Forest Machine Learning (RFML) is one of the ensemble-based machine learning techniques (Rahaman et al., 2019), with prevalent applications in classification and regression problems (Breiman, 2001). It generates a set of decision trees using homogenous subsets of random predictors (Rahaman et al., 2019). The downscaling model was organized and implemented as follows: (i) The training data including surface topography, soil moisture, snow water, rainfall, runoff, temperature, and evapotranspiration, were aggregated to 25 km using bilinear interpolation method similar to the GRACE's spatial resolution, and consequently their associations with TWSA values were examined. Later, the RFML model was applied for TWSA predictions at coarse resolution (25 km). (ii) The TWSA residuals at the same resolution (25 km) were estimated by deducing the RFML-predicted TWSA from the GRACE-derived TWSA. (iii) Then, the trained RFML model was applied to the input variables at a spatial resolution of 1 km to obtain fine-resolution TWSA estimates. At the final stage, the residuals interpolated at 1 km using bilinear interpolation method were added to the estimated 1 km TWSA to obtain the downscaled TWSA over the KB.

K-fold cross-validation was employed to assess the robustness of the RFM (Ali et al., 2021). The k-fold cross-validation technique partitions the data set into k subsets and utilizes different subsets for training the model while using the remaining examples for testing. This approach allows for a comprehensive evaluation of the model's performance across numerous train and test samples. It is conventional to employ a 10-fold cross-validation technique and thereafter compute the average of the obtained results, so enhancing the reliability of the findings.

2.3.2 | Water storage deficit index

Water storage deficit index (WSDI) (Thomas et al., 2014) was utilized for drought evaluation in the study area. To calculate the WSDI, water storage deficit (WSD) values were first calculated based on Equation (2) by subtracting the climatology (long-term monthly) values of TWSA from the TWSA time-series. Then, the WSDI was extracted by standardizing the computed WSD based on Equation (3) by using the mean and the standard deviation of the WSD time-series.

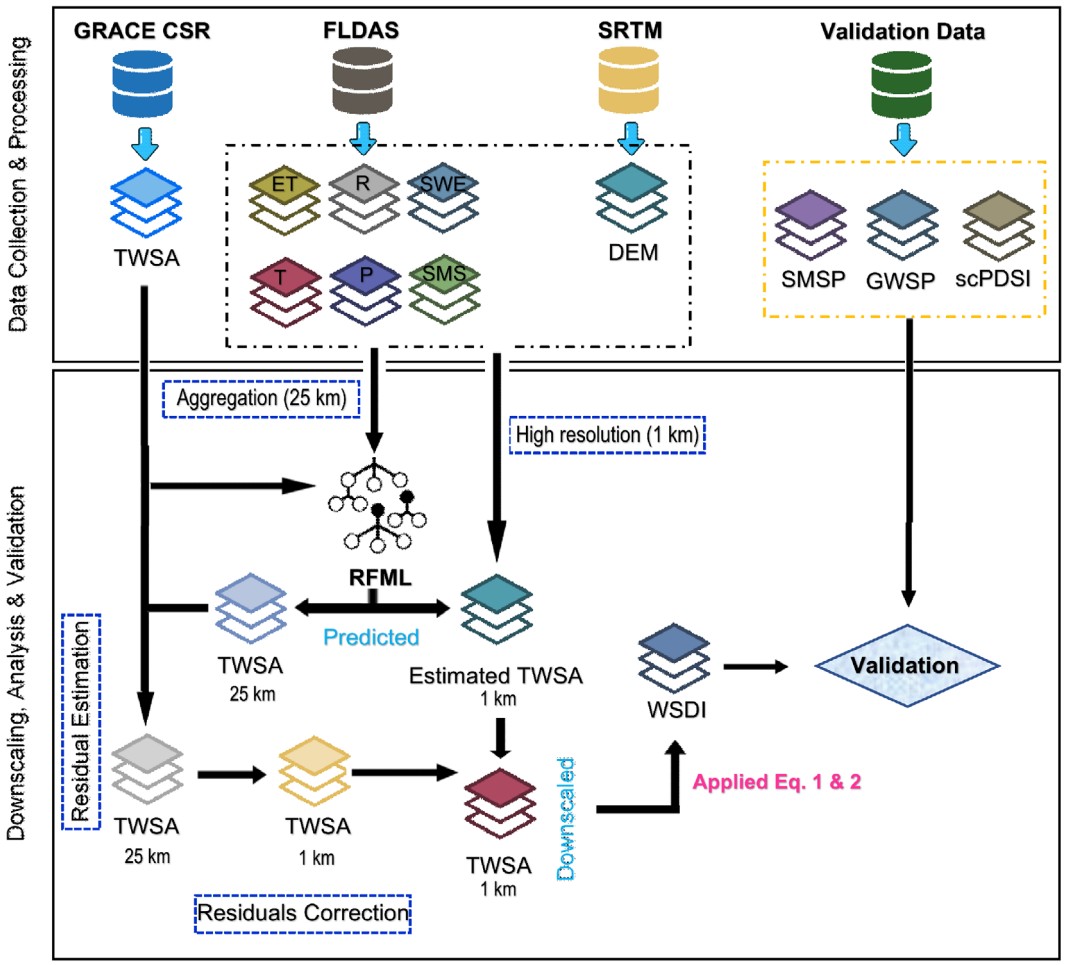

FIGURE 2 The schematic flow of the analysis.

$$WSD_{i,j} = TWSA_{i,j} - \overline{TWSA_j}, \quad (2)$$

$$WSDI = \frac{WSD_{i,j} - \bar{x}_{WSD}}{\bar{s}_{WSD}}, \quad (3)$$

where $TWSA_{i,j}$ and $WSD_{i,j}$ are the downscaled-based *TWSA* and total WSD time-series for the *j*th month in the year *i*, respectively; $\overline{TWSA_j}$ is the long-term mean of *TWS* for the corresponding month (the *j*th month in a year *i*), $\bar{s}_{WSD}$ and $\bar{x}_{WSD}$ are the standard deviation and mean of the WSD time-series, respectively.

Water deficit or surplus conditions of a given area is determined according to the sign of the WSD. Negative and positive values of WSD demonstrate water storage shortage and surplus respectively. The duration of negative WSD values over a region is a clear indication of a drought incident. The persistence of negative WSD values for three or more consecutive months over a region indicates the existence of a drought event (Thomas et al., 2014). The monthly departures from the average situation of the region in each month are represented as the WSDI time-series and may be used as a proxy for the severity of drought.

The drought severity was evaluated using Equation (4) (Thomas et al., 2014) through which the combined effects of water storage deficit and drought duration are taken into account.

$$Se(t) = M(t) \times D(t), \quad (4)$$

where, *Se* depicts the drought severity, of the number of droughts (*t*). M and *D* represent the average storage deficit and the drought duration respectively. In comparison to the WSD, this approach is very effective in illuminating droughts due to its capability of integrating the WSD with drought duration. The WSD is a useful variable only when the WSDI has identified a specific drought in a region and the previous month's value indicates the severity of that event. The drought classes based on the WSDI are given in Table S4.

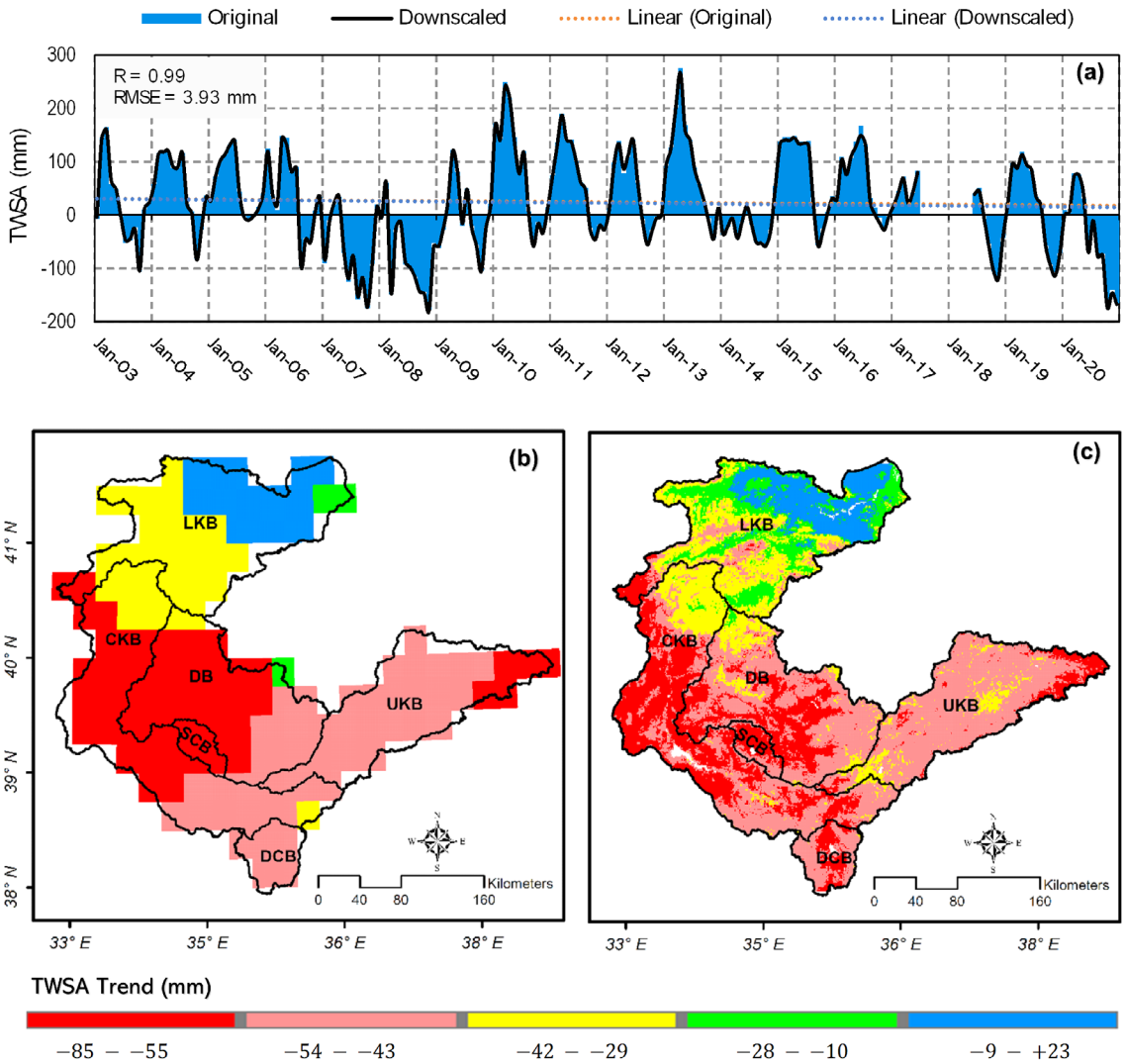

FIGURE 3 (a) Time-series associations between the GRACE-derived TWSA (25 km), and the downscaled TWSA (1 km) and the spatial fluctuations of TWSA in 2020 before (b), and after (c) downscaling from 2003 to 2020.

A brief description of the methodological flow of the analysis is given in Figure 2. Overall, the analysis consists of several stages. First, RFML model was developed to predict the finer resolution of the GRACE-like TWSA estimates using some fine resolution hydro-climatic parameters received from the FLDAS model. Second, the WSDI was estimated using the downscaled TWSA based on Equations 1 and 2. And finally, the validation and interpretation of the results were done using auxiliary information received from some open-source data sets such as scPDSI, SMSP, and GWSP.

3 | RESULTS

3.1 | Downscaling performance

As the first step of the analysis, the original TWSA estimates with a resolution of 25 km were downscaled to a 1 km data set based on the RFML algorithm. The downscaled and the original TWSA time-series were evaluated to assess the performance of the downscaling model. The TWSA time-series (Figure 3a) demonstrates a very well performance for the downscaling model in catching the fine resolution fluctuations of the original TWSA with high R^2 (0.99) and low RMSE (3.93 mm). The good performance of the RFML model found in this study agrees well with the findings of some researchers. For instance, Ali et al. (2021), Khorrami (2023), and Chen et al. (2019) reported high correlation values of 0.97, 0.87, and 0.83, respectively between the RFML-based downscaled and GRACE-based TWSA time-series. To provide a better illustration of the model performance, the spatial distribution of the TWSA values over the KB was depicted before and after downscaling in Figure 3b and c, respectively.

3.2 | Fluctuations of terrestrial water storage

The basin-average time-series of precipitation and the fine resolution TWSA were generated to investigate their monthly fluctuations, as well as their associations over each subbasin of the KB (Figure S1). According to the results, the fluctuations of TWSA in the LKB are ascending, while the remaining subbasins demonstrate diminishing water storage. The results also reveal that during the years 2007, 2008, 2018, 2019, and 2020, all the studied subbasins suffered from critical water storage anomalies. This dry situation is particularly exacerbated in 2008 and 2020, during which all the subbasins of the study area lost most of their water storage. March 2008 was the most critical time in the last 18 years in which the LKB lost an estimated water storage of −383.57 mm. The remaining subbasins show different times of maximum storage loss. The results show that the DCB, SCB, UKB, CKB, and DB respectively lost −253.11 mm (November 2020), −214.20 mm (November 2020), −207.80 mm (November 2008), −188.91 mm (December 2020), and −187.86 mm (November 2008). The acute depletion of water storage in the KB is a local footprint of the widespread droughts striking Türkiye during the dry years of 2007 to 2008 and 2018 to 2020 (Khorrami & Gunduz, 2021b; Okay Ahi & Jin, 2019).

Conversely, an unremitting pluvial period is seen for all the studied subbasins from 2010 to 2013 during which water storage of the basins manifests an increasing trend, especially in April 2013, when the water storage of the basins set a record during the GRACE era. According to the results, the maximum number of wet months (139 months) is seen in the LKB which accounts for 64% of the total study months. The maximum number of dry months (113), on the other hand, belongs to the DCB accounting for 52% of the study months. Therefore, it can be stated that the LKB and DCB are the wettest and driest basins from the perspective of the temporal fluctuations of TWSA.

TABLE 1 Trend analysis results of the basin-wise Terrestrial Water Storage Anomalies (TWSA) and Precipitation (P).

Parameter	Basin name	Trend			*p*-value	MK trend test ($\alpha = 0.05$)
		mm/year	km^3/year	Total change (km^3)		
Terrestrial Water Storage Anomalies	LKB	+3.51	+0.075	+1.36	0.002	Ascending trend[a]
	CKB	−1.15	−0.025	−0.45	0.105	Descending trend
	DB	−1.14	−0.020	−0.35	0.087	Descending trend
	UKB	−1.58	−0.025	−0.46	0.036	Descending trend[a]
	DCB	−2.34	−0.007	−0.12	0.002	Descending trend[a]
	SCB	−1.31	−0.002	−0.03	0.035	Descending trend[a]
Precipitation	LKB	+1.21	+0.026	+0.47	0.225	Ascending trend
	CKB	+0.23	+0.005	+0.09	0.822	Ascending trend
	DB	−3.18	−0.055	−0.98	0.001	Descending trend[a]
	UKB	−0.61	−0.010	−0.18	0.544	Descending trend
	DCB	+0.45	+0.001	+0.02	0.649	Ascending trend
	SCB	−1.21	−0.002	−0.03	0.225	Descending trend

[a]Statistically significant.

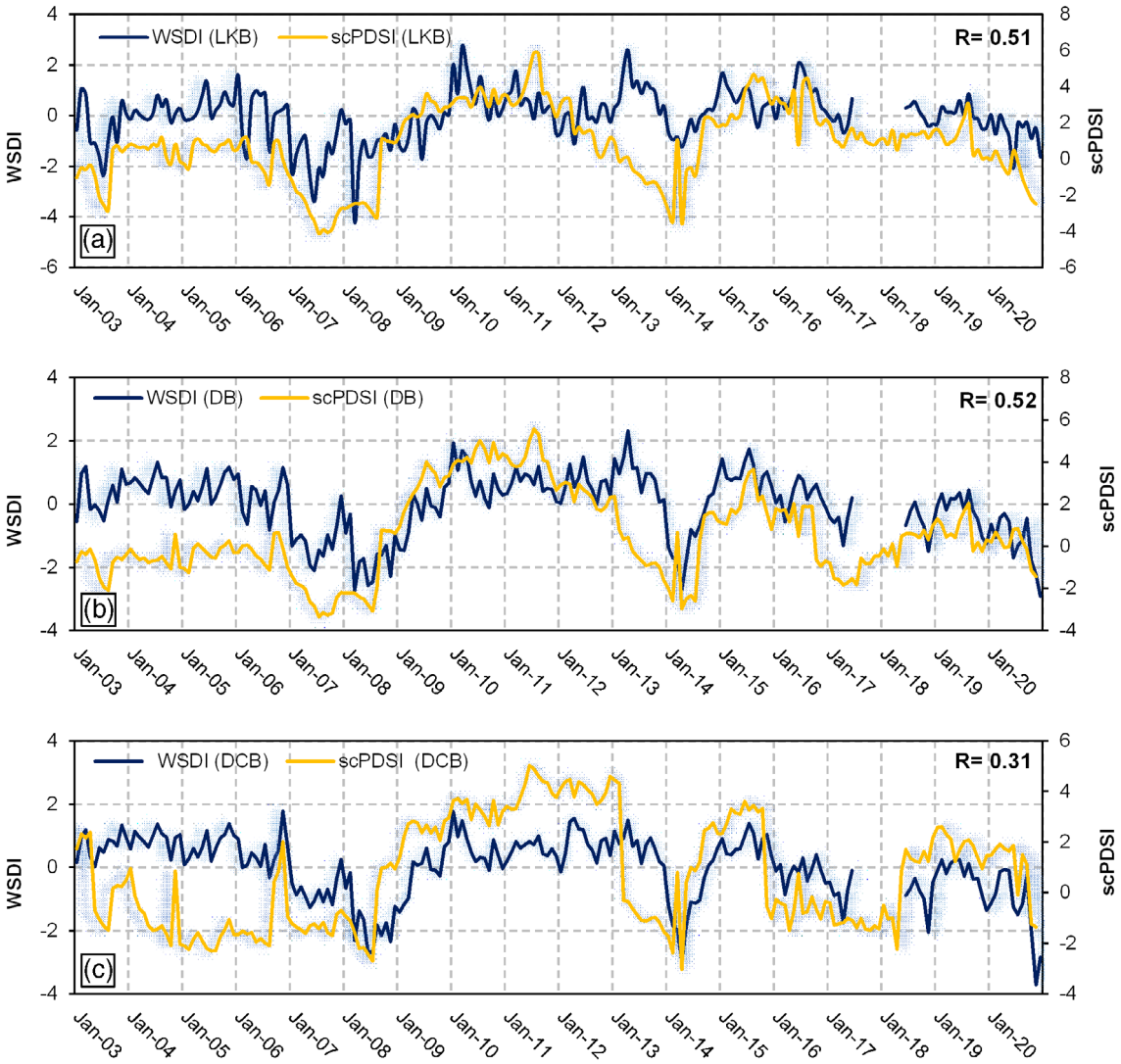

FIGURE 4 Temporal interactions between the water storage deficit index (WSDI) and self-calibrated palmer drought severity index (scPDSI) over LKB (a), DB (b), DCB (c), CKB (d), SCB (e), and UKB (f).

The monthly variations of precipitation, on the other hand, demonstrate ascending trends for the LKB, DCB, and CKB subbasins while the DB, UKB, and SCB manifest an increasing trend during the same time. The temporal fluctuations of the precipitation and TWSA are of moderate associations ranging from 0.30 (over the LKB) to 0.48 (over DCB and UKB), which may stem from the existing temporal lag between them over almost all the studied subbasins. The time-series analysis also reveals that, on average, the LKB, DB, DCB, CKB, SCB, and UKB have suffered from the least received annual precipitation of about 47 mm (2018), 28 mm (2016), 33 mm (2017), 25 mm (2016), 30 mm (2008), and 30 mm (2013), respectively.

The long-term monthly (climatology) fluctuations of TWSA and precipitation are given in Figure S3. According to which, the minimum amount of precipitation was observed in the study area during August, September, and October. The decreasing precipitation during this period corresponds to the diminishing water storage of the basins, which culminates in the least recorded amount of TWSA in October for all the subbasins. The climatology associations between TWSA and precipitation indicate a powerful link between them where the correlation values range from 0.71 (over the SCB) to 0.79 (over LKB).

3.3 | Trend analysis results

The MK trend test and Sen's slope technique were applied to determine precipitation and TWSA trends over each subbasin at the significance level of 0.05 (Table 1). According to the results, the storage of the LKB has been augmented by +3.51 mm per annum which is equivalent to 1.36 km^3 of total storage surplus. However, the remaining basins have suffered from declining water reserves, among which DCB has been the most critical basin, where the basin storage has been reduced by −2.34 mm per annum.

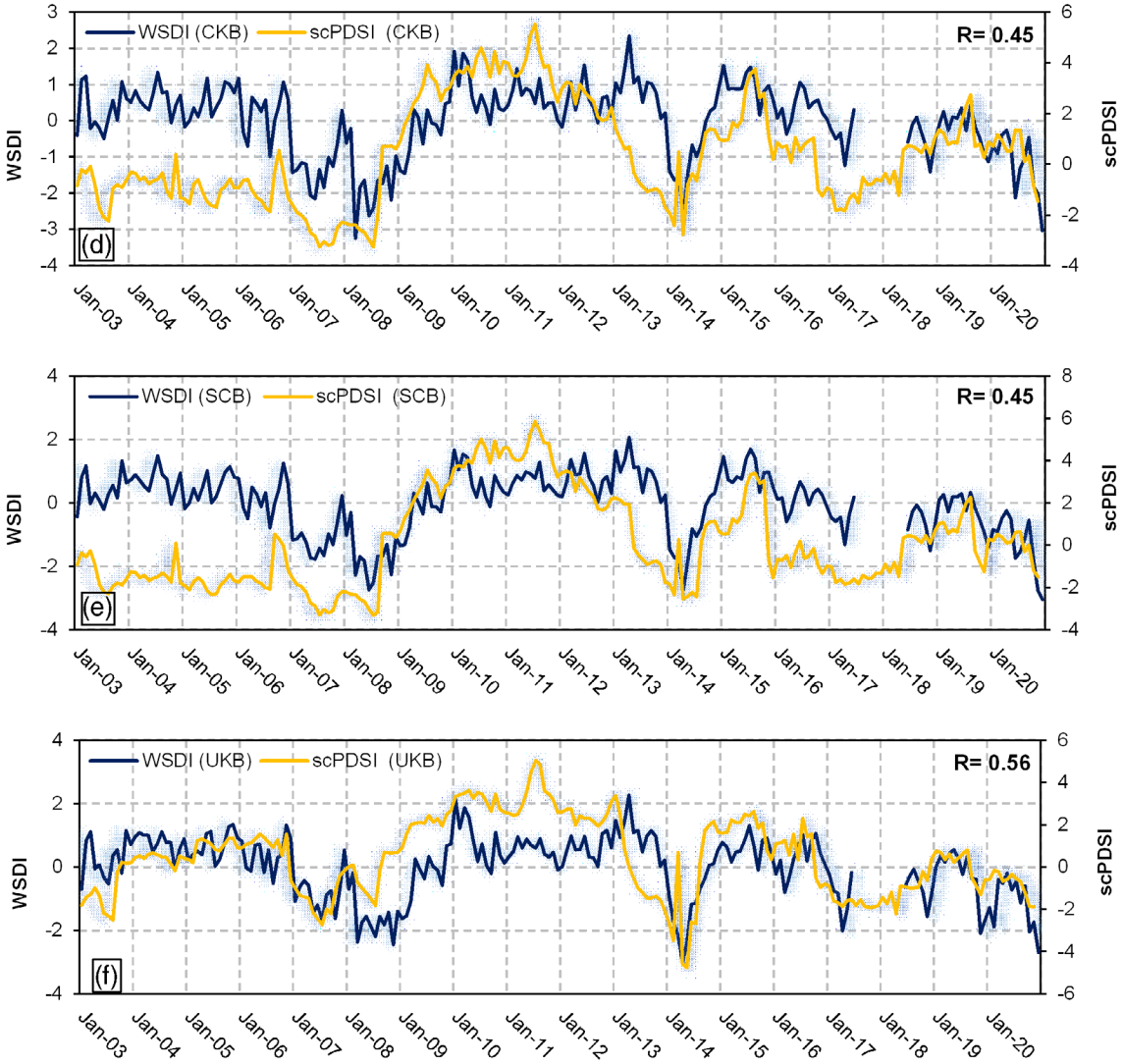

FIGURE 4 (Continued)

The precipitation time-series, on the other hand, reveals that while there is a diminishing trend for the DB (−3.18 mm/year), UKB (−0.61 mm/year), and SCB (−1.21 mm/year), an ascending trend is observed for the LKB (+1.21 mm/year), CKB (+0.23 mm/year), and DCB (+0.45 mm/year). The significance test analysis results suggest that except for the DB with a significant decreasing P trend, the estimated trends of the remaining subbasins are not statistically significant.

3.4 | Associations between WSDI and drought indices

The temporal variations in WSDI were evaluated and validated against the variations of other drought indicators including the scPDSI, SMSP, and GWSP.The temporal associations between WSDI and scPDSI (Figure 4) manifest a generally good agreement over almost all the subbasins. Except in the DCB, for which the correlation is 0.31, the WSDI in LKB, DB, CKB, SCB, and UKB show relatively good performance with a correlation of 0.51, 0.52, 0.45, 0.45, and 0.56, respectively. It is observed that there was a relatively low to moderate agreement between the WSDI and scPDSI in the subbasins of the KB. However, the WDSI was successful in catching the descending trend of the scPDSI during the drought events in 2007–2008, 2014, and 2018–2020. Therefore, it can be stated that the WSDI can detect and trace dry periods over small-scale areas.

The associations between WSDI and the simulated drought indicators of SMSP and GWSP are illustrated in Figures 5 and 6, respectively. According to the results, there is overall a higher agreement for the WSDI-SMSP and WSDI-GWSP interactions than WSDI-scPDSI in the studied subbasins. The correlation for the WSDI-SMSP over LKB, DB, DCB, CKB, SCB, and UKB is 0.60, 0.59, 0.58, 0.60, 0.61, and 0.62, respectively. The temporal associations are even stronger for the WSDI-GWSP relation with a correlation of 0.71 (over LKB), 0.77 (over DB), 0.79 (over DCB), 0.78 (over CKB), 0.79 (over SCB), and 0.81 (over UKB). The strong agreement observed for the CLSM-derived SMSP and GWSP with the WSDI is justifiable because the

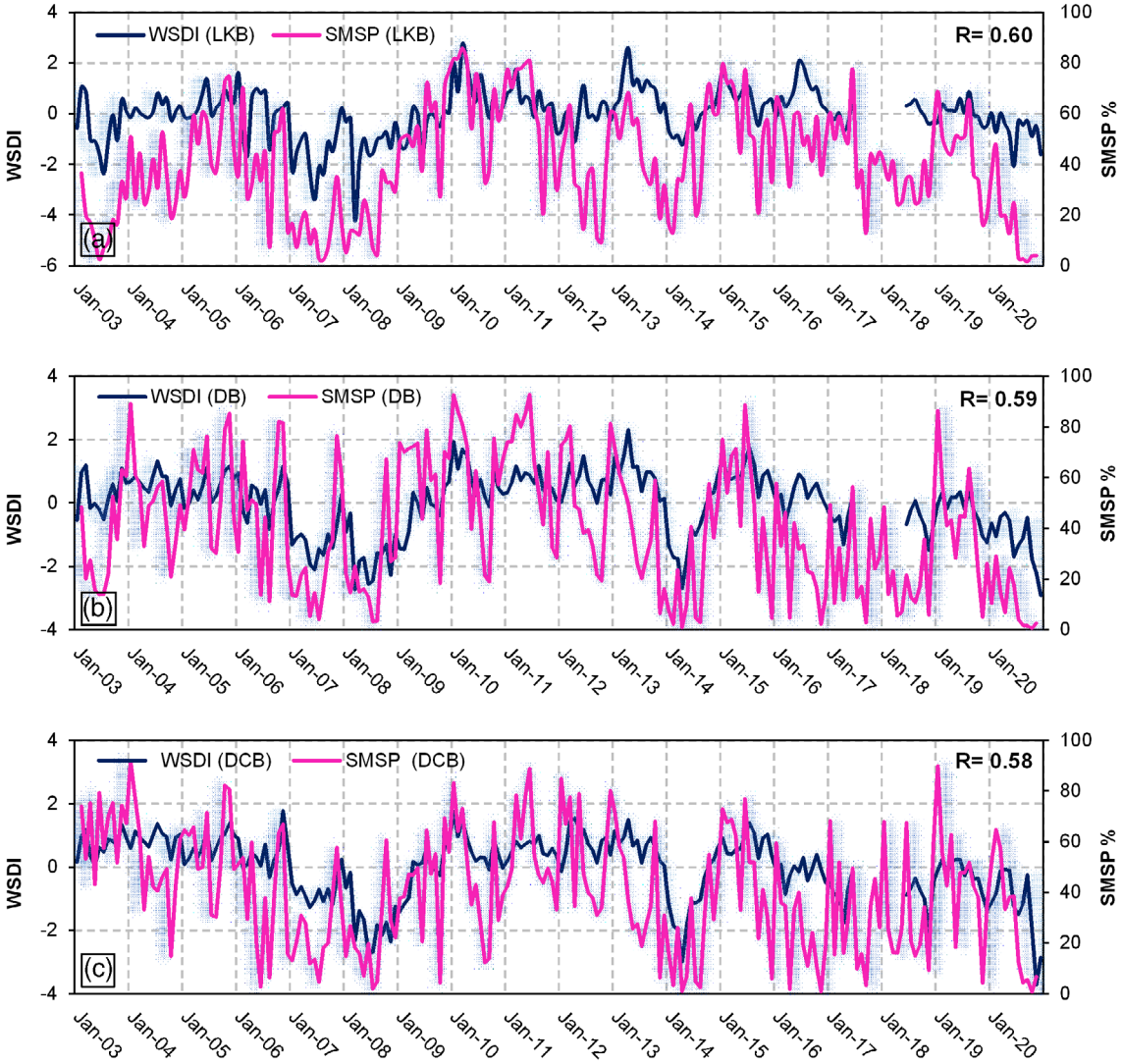

FIGURE 5 Temporal interactions between the water storage deficit index (WSDI) and soil moisture storage percentile (SMSP) over LKB (a), DB (b), DCB (c), CKB (d), SCB (e), and UKB (f).

CLSM model uses the GRACE data to improve its estimates through sophisticated data assimilation models (Li & Rodell, 2015). Therefore, the drought indices derived based on this approach yield more accurate results.

The spatial correlation maps (Figure 7) illustrate the spatial patterns of the correlation values of the WSDI and the other indices over the KB basin. According to Figure 7-a, the spatial agreement between the WSDI and scPDSI ranges from 0.31 to 0.56 with the maximum correlation seen over the LKB, DB, and a part of UKB subbasins. The spatial correlation between the WSDI and SMSP (Figure 7-b) is above 0.50 for the whole area with the maximum agreement over the SCB, DB, and UKB. The best spatial association is observed between the WSDI and GWSP (Figure 7c) ranging from 0.53 to 0.82. The southern and western subbasins of UKB, DB, SCB, and the majority of CKB manifest the highest spatial association between the WSDI and GWSP.

3.5 | Drought characterization based on drought indices

The drought events of the study area were categorized based upon the used indices of the WSDI, scPDSI, SMSP, and GWSP according to corresponding tables of classification given in Data S1. The lower WSD and longer duration were considered to define the harshness of the drought events. Accordingly, two harshest droughts were identified for all the subbasins of the KB. The first event was observed between January 2008 and March 2009 (15 months in duration). The second event was observed from September 2019 to December 2020 (16 months in duration). Although Türkiye experienced a country-wise dry period in 2014 (Khorrami & Gunduz, 2021a), the analysis results suggest that it has had a trivial short-term impact on the water storage of the KB compared to the droughts that transpired in the above-mentioned periods. The characteristics of the detected droughts are

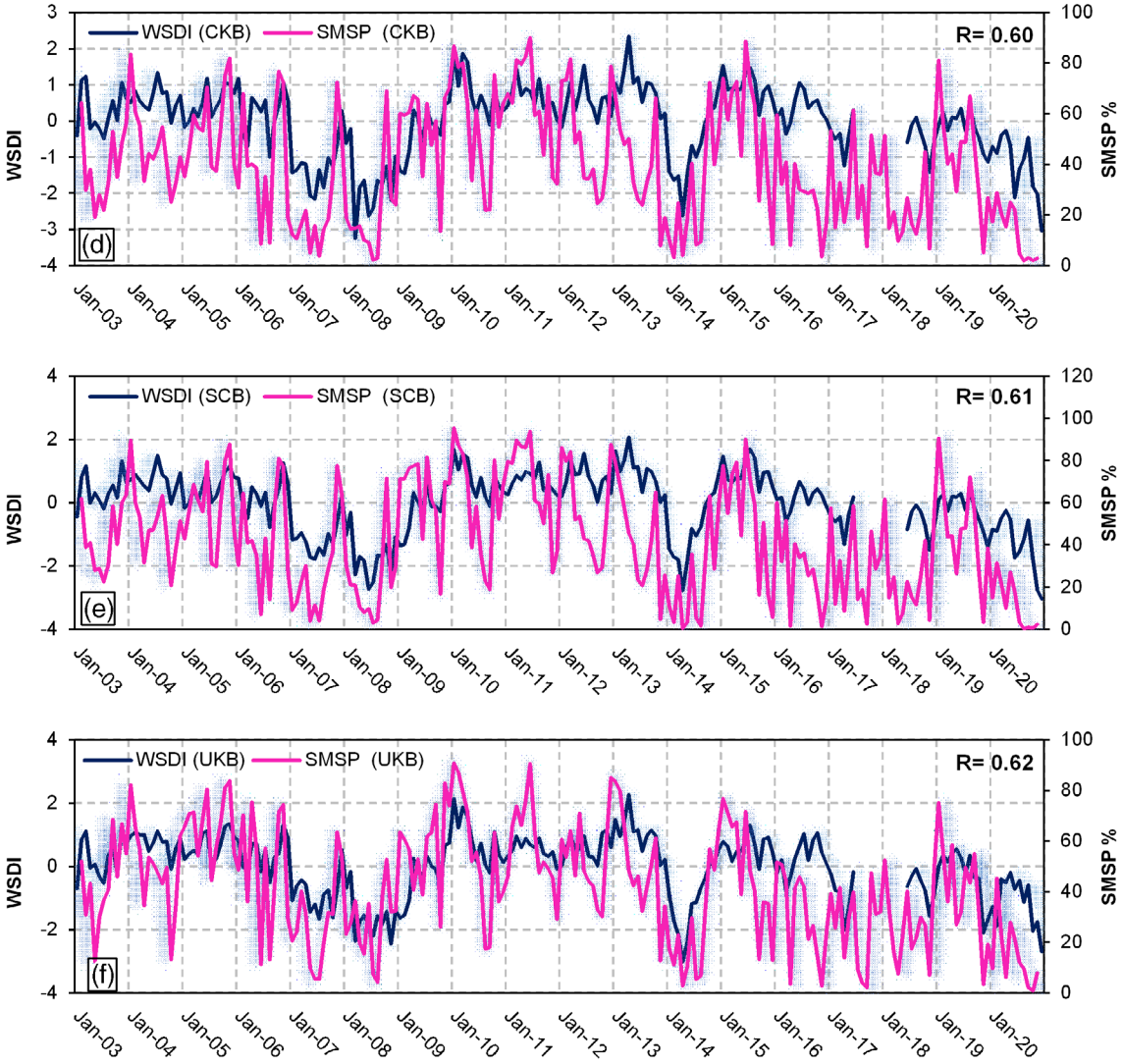

FIGURE 5 (Continued)

given in Table 2, according to which the most critical situation in terms of hydrological severity is observed in the LKB basin with a total storage loss of about 2053 and 1010 mm during the first and the second harsh drought incidents. The LKB is followed by DCB, DB, SCB, CKB, and UKB with a total storage loss of 1368, 1331, 1286, 1116, and 1142 mm, respectively during the first dry period. But for the second dry period, the LKB is followed by SCB, DCB, DB, UKB, and CKB with the estimated storage loss of 1002, 991, 965, 882, and 821 mm, respectively.

From the perspective of the maximum water storage losses during the discerned dry periods, it can be stated that March 2008, and December 2020 have been the most critical months, during which the majority of the study subbasins have experienced peak water deficits. According to Table 2, the LKB has the most dramatic situation in terms of the experienced peak storage deficit that happened in March 2008 (−466.07 mm) and in Jun 2020 (−229.85 mm). The UKB, on the other hand, manifests the least peak deficit recorded in November 2008 (−118.78 mm) and in December 2020 (−131.05 mm).

The drought categorization into different levels was done considering the defined levels of severity for each drought index given in Tables S2, S3, and S4. Except for the drought indices of WSDI and GWSP, with almost identical drought classes during the drought incidents, trivial discrepancies are seen in the severity level of droughts based on different indicators. The classification of drought severity is given in Table 3. According to the results, it is revealed that notwithstanding the contrasts in the severity levels among drought indices, there is more consistency in terms of the detected droughts during the second dry period (September 2019–December 2020) than during the first period (January 2008–March 2009). The consistency of the results during the second drought incident is even more noticeable for the WSDI, SMSP, and GWSP over the DB, CKB, DCB, SCB, and UKB with the ascribed 'moderate' drought category. While the scPDSI discloses the existence of a 'mild' situation for all the subbasins excluding the LKB and SCB with 'moderate', and 'normal' situations, according to SMSP, and GWSP, the drought severity was of 'moderate' class for all the study area during the second dry period.

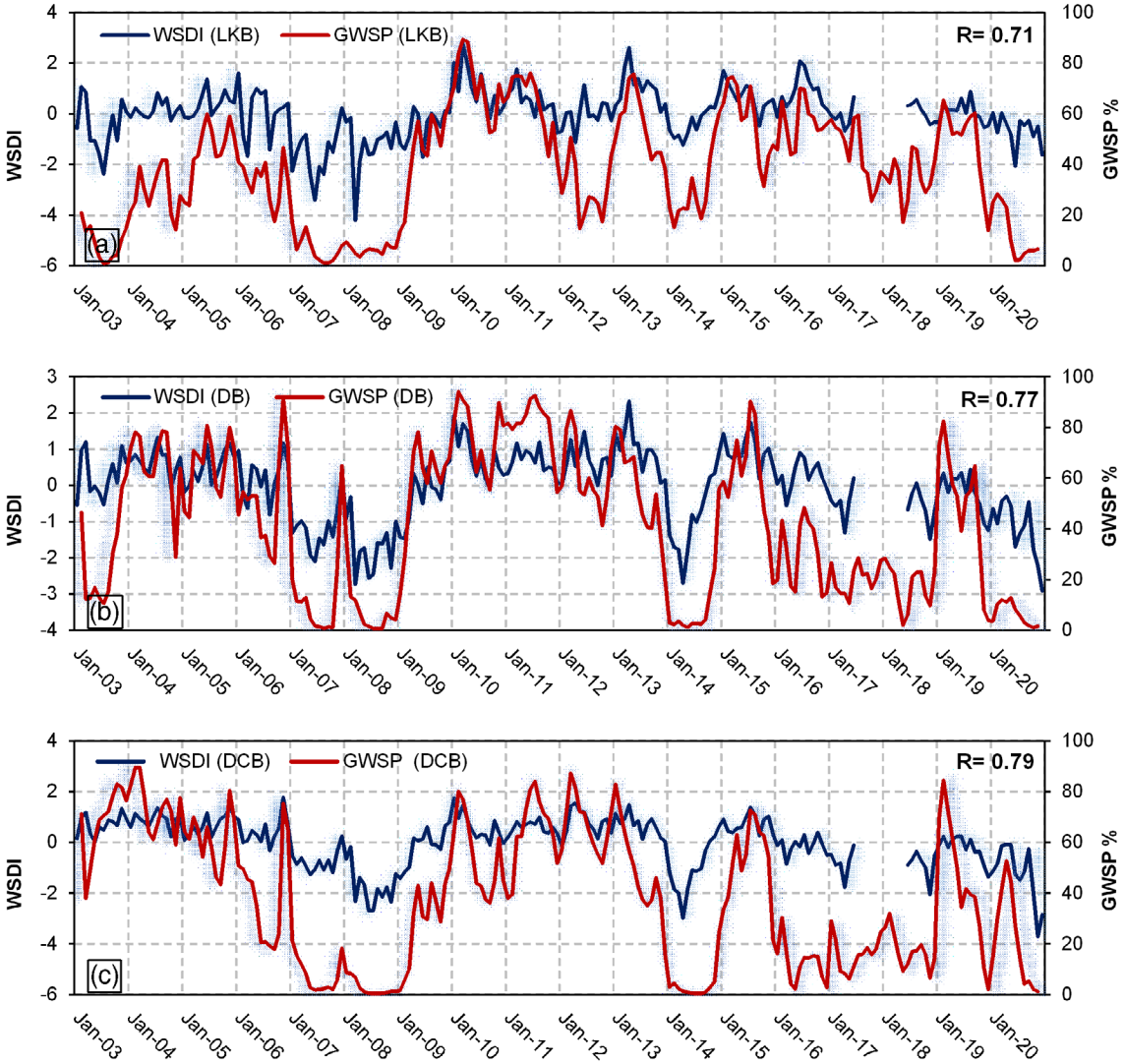

FIGURE 6 Temporal interactions between the water storage deficit index (WSDI) and groundwater storage percentile (GWSP) over LKB (a), DB (b), DCB (c), CKB (d), SCB (e), and UKB (f).

During the first period, however, the inconsistency between the severity levels of drought over the subbasins of the study area is more profound. WSDI demonstrates a 'moderate' drought period for all the subbasins, the scPDSI, on the other hand, indicates a 'mild' situation for almost all the subbasins. This inconsistency is more evident between the SMSP- and GWSP-based categorized droughts. According to the SMSP, there is an 'abnormal' drought over the subbasins in the first drought period. However, the GWSP manifests an 'extreme' drought for the DCB, a 'severe' drought for the CKB, and a 'moderate' drought for the DB, SCB, and UKB. Overall, a maximum difference of one severity level was observed between the drought indices over the majority of the subbasin of the KB. The characterization of drought based on different indices revealed discrepancies in the severity of the droughts. The discrepancies observed between the drought classes based on the used indices may be ascribed to the differences in hydrological ingredients and used algorithms as well (Cui et al., 2021). While the WSDI represents a combined set of different hydrological components such as the water input and output (Emerton et al., 2016), scPDSI takes into account only a handful of those data such as precipitation (Sinha et al., 2017).

3.6 | Drought spatial variability

The drought was further evaluated in a spatial context by using the thematic maps of WSDI. As the most dramatic drought event over the KB from 2003 to 2020, the first drought incident (January 2008–March 2009) was selected to be evaluated spatially. To this end, the drought incident over the KB was portrayed spatially based on the monthly WSDI values (Figure 8). According to the results, it is observed that the most drought-beaten part of the KB is the northern part over the LKB. While the LKB has the most dramatic situation, the UKB in the Eastern KB turns out to suffer less from the drought incident. However, in January 2008 and December 2008, there is a

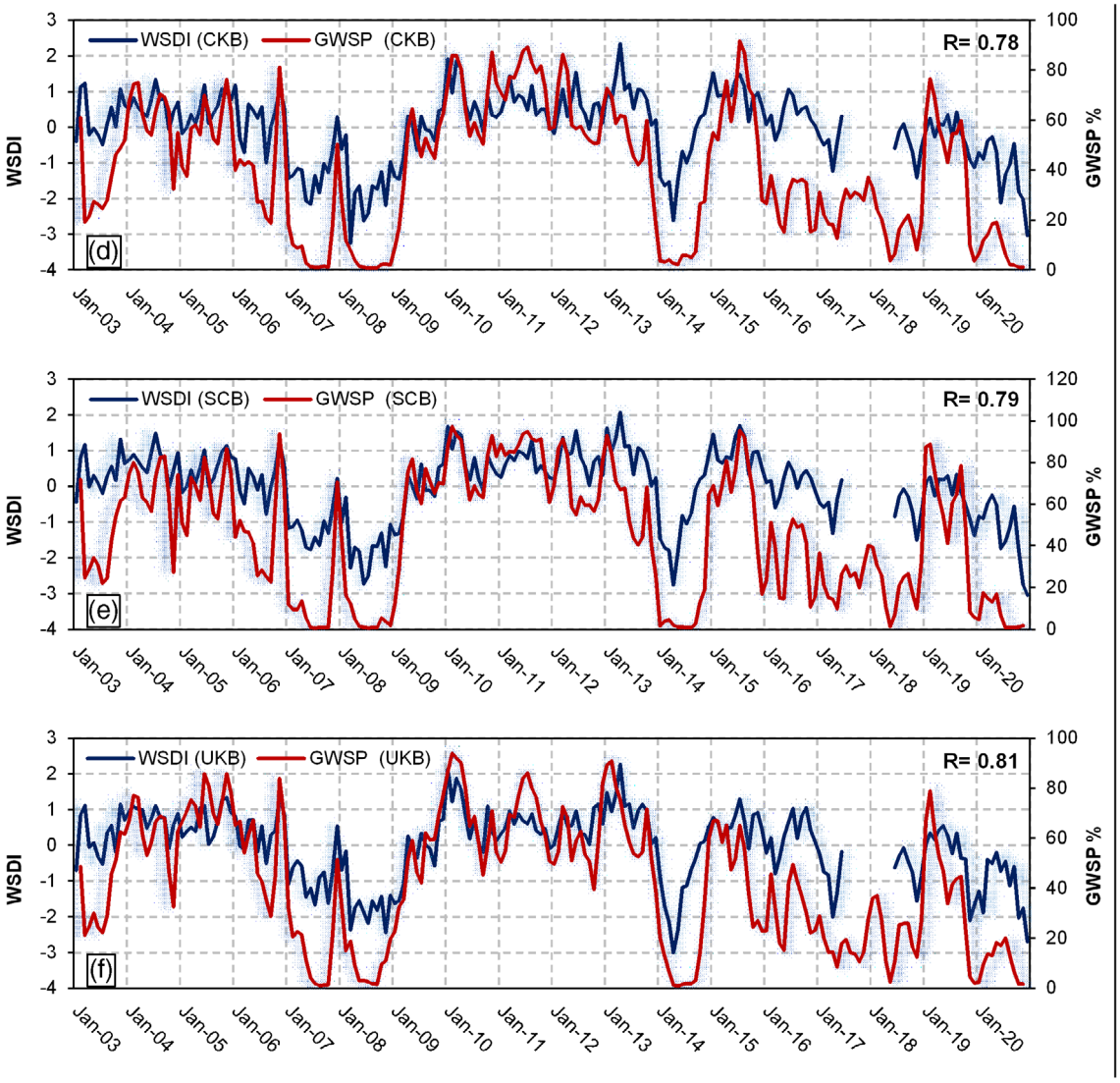

FIGURE 6 (Continued)

different spatial pattern of the WSDI, during which the majority of the KB is covered by the lower WSDI values suggesting a basin-wide drought incident on these dates.

The map of the drought-ravaged areas demonstrates the drought development and its impacted regions with various intensities. Figure 9 illustrates the geographical evolution of WSDI in different subbasins of the KB during 2003–2020. The area percentage of the drought-beaten subbasins is given based on the monthly droughts of various severity levels to more clearly identify the regions affected by various levels of drought. According to the results, the first drought incident (January 2008 – March 2009) affected about 37%,46%,49%,53%,56%, and 65% of the area of LKB, DB, CKB, DCB, SCB, and UKB subbasins, respectively. The above-mentioned subbasin has also suffered from extreme drought (IV) during the same period with an area percentage of 15%,0.08%,3%,1%,0.7%, and 0.01%, respectively. During the second incident (September 2019 – December 2020), drought has beaten the LKB, DB, CKB, DCB, SCB, and UKB subbasins with the estimated area percentage of 52%,62%,63%,59%,62%, and 61%, respectively. During this period the extreme drought overtly impacted the LKB, and CKB with the affected area of 6.5% and 3%, respectively. The DB and DCB were slightly subjected to extreme drought with the affected area of 0.23% and 0.66%, respectively. The impact of the transpired extreme drought during this dry period was trivial over the SCB and UKB. A summary of the drought area percentages is given in Table 4.

4 | DISCUSSION

4.1 | WSDI performance

Drought incidents can be more effectively determined and surveyed by using the drought indices derived from the GRACE/GRACE-FO observations compared to the traditionally used standardized drought

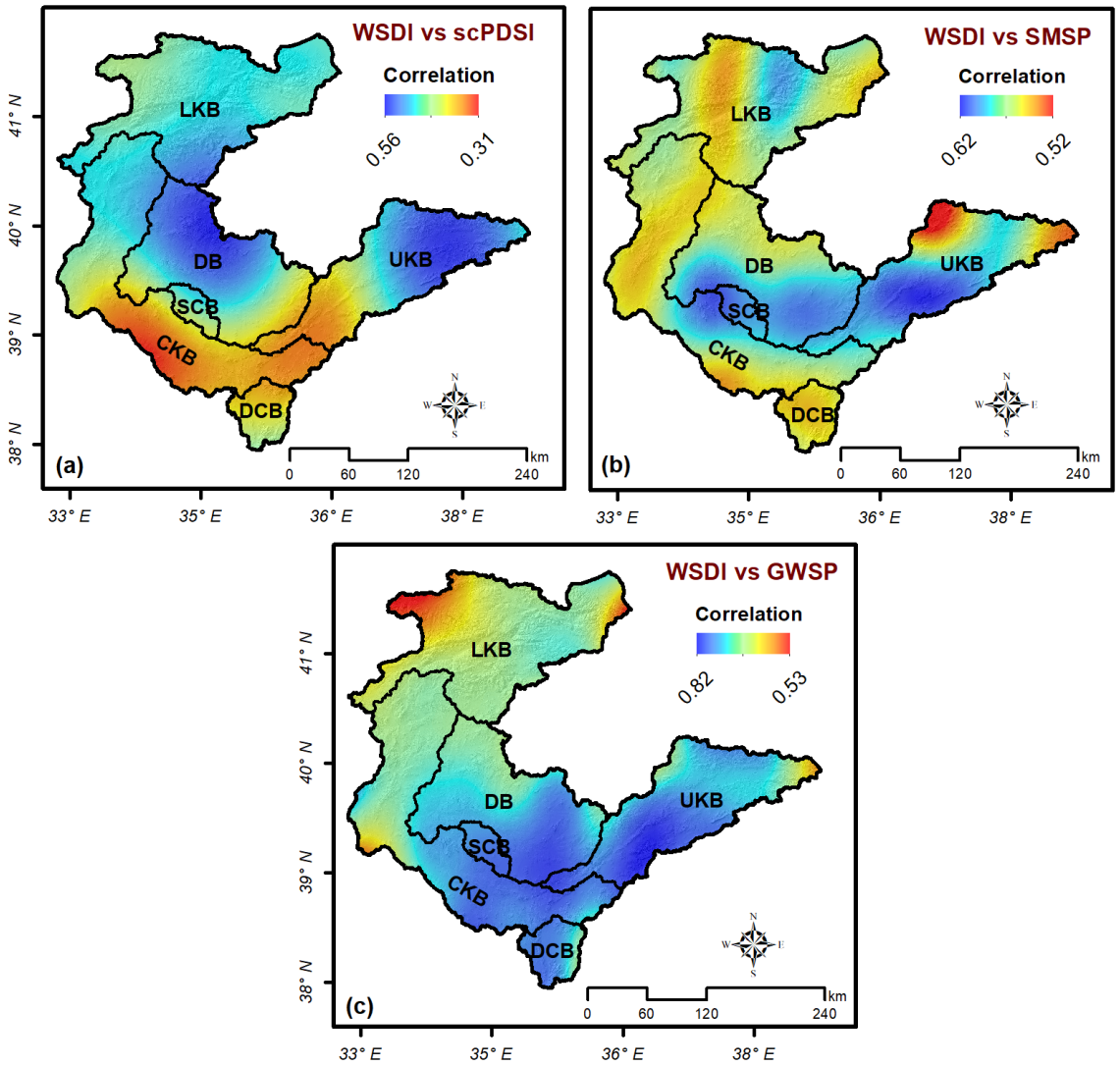

FIGURE 7 Spatial association of the time series drought indices from 2003 to 2020 over the KB. WSDI versus scPDSI (a), WSDI versus SMSP (b), and WSDI versus GWSP (c).

indicators (Nigatu et al., 2021). The GRACE project is adept at detecting hydrological extremes because they vertically integrate the storage variations from the surface to the deep layers of aquifers. Thus, they can potentially detect the water storage loss of surface water, shallow groundwater, and deep groundwater (Cui et al., 2021). Since traditional drought indices depend on the accumulation of rainfall deficits, they are usually lame in describing droughts and their impact on the hydrological system of subsurface structures. (Thomas et al., 2014). As an enhanced form of PDSI, the scPDSI does also account for the net water changes but through a simplified model, which usually represents the water balance of shallow soil depth (Zhao, Geruo, et al., 2017). The sc-PDSI is more suitable to characterize just agricultural droughts. Additionally, it is weak in quantifying drought trends and magnitude in drier regions (Xu et al., 2021). From this perspective, the tenuous connection between the time-series of the TWSA-based WSDI and scPDSI can be rationalized. The major reason is that the TWSA-identified droughts and meteorological droughts are different in timing due to the inherent lags within the hydrologic system (Thomas et al., 2014). Moreover, traditional indices depend mainly on hydro-climatic variables and fluxes with a trivial impact on the top surface system. However, differences in the subsurface system characteristics may also play a paramount role in the formation of drought, especially for prolonged and extremely intense droughts. Conversely, by integrating the effects of multiple surface and subsurface hydrological phenomena, the Water Storage Deficit Index (WSDI) can accurately measure the amount of water that is depleted from storage. Furthermore, the sensitivity of the scPDSI to strong meteorological droughts is low compared to other indices (Van der Schrier et al., 2011). Although the scPDSI has contributed a lot to improving spatial consistency and controlling the frequency of extreme incidents (Trenberth et al., 2014), it is more sensitive to extreme variations in the surface soil moisture (Van der Schrier et al., 2011).

The WSDI shows strong accordance with the CLSM-derived drought indices of SMSP and GWSP, which is justifiable because the

TABLE 2 Characteristics of the most severe droughts discerned based on the fluctuations of TWSA.

Period (duration)	Subbasin	Average deficit (mm)	Total severity (mm)	Peak deficit (mm)
Jan 2008–Mar 2009 (15 months)	LKB	−136.9	−2053.8	−466.1 (Mar 2008)
	DB	−88.7	−1330.8	−150.9 (Mar 2008)
	CKB	−74.4	−1116.2	−123.2 (Jun 2008)
	DCB	−91.8	−1367.7	−184.3 (Mar 2008)
	SCB	−85.8	−1286.5	−147.4 (Jun 2008)
	UKB	−76.1	−1141.8	−118.8 (Nov 2008)
Sep 2019–Dec 2020 (16 months)	LKB	−63.2	−1010.5	−229.8 (Jun 2020)
	DB	−60.3	−965.2	−160.8 (Dec 2020)
	CKB	−51.3	−820.9	−169.9 (Nov 2020)
	DCB	−61.9	−990.9	−172.9 (Dec 2020)
	SCB	−62.6	−1001.7	−164.3 (Dec 2020)
	UKB	−55.1	−881.9	−131.1 (Dec 2020)

TABLE 3 Classification of the most severe droughts discerned based on drought indicators.

		Grade			
Period (duration)	Subbasin	WSDI	sc-PDSI	SMSP	GWSP
Jan 2008–Mar 2009 (15 months)	LKB	III (moderate)	III (moderate)	I (abnormal)	III (severe)
	DB	III (moderate)	II (mild)	I (abnormal)	II (moderate)
	CKB	III (moderate)	II (mild)	I (abnormal)	III (severe)
	DCB	III (moderate)	II (mild)	I (abnormal)	IV (extreme)
	SCB	III (moderate)	II (mild)	I (abnormal)	II (moderate)
	UKB	III (moderate)	I (normal)	I (abnormal)	II (moderate)
Sep 2019–Dec 2020 (16 months)	LKB	II (mild)	III (moderate)	II (moderate)	II (moderate)
	DB	III (moderate)	II (mild)	II (moderate)	II (moderate)
	CKB	III (moderate)	II (mild)	II (moderate)	II (moderate)
	DCB	III (moderate)	II (mild)	I (abnormal)	II (moderate)
	SCB	III (moderate)	II (mild)	II (moderate)	II (moderate)
	UKB	III (moderate)	II (mild)	II (moderate)	II (moderate)

CLSM model has integrated the GRACE data into its simulations to improve their quality (Li & Rodell, 2015; Zaitchik et al., 2008). The enhanced CLSM-derived drought indicators, ought to give a more comprehensive and objective characterization of droughts (Rui et al., 2018). Furthermore, the GRACE signals are more sensitive to the surface and subsurface water storage anomalies (Scanlon et al., 2016), thus, they supply realistic information on the soil moisture and groundwater conditions at depth. Therefore, the drought indices derived from the TWSA data are more likely to agree with the soil moisture- and groundwater storage-related drought indices such as the SMSP and GWSP. Because the GRACE TWSA encompasses various components of the hydrological water cycle (Longuevergne et al., 2013), the GRACE is potent enough to capture the storage dynamics in deep soil water as well as groundwater (Wang & Pozdniakov, 2014). The SMSP and GWSP represent the water storage status of the surface soil and groundwater aquifers. Considering the strong association between the WSDI and GWSP, it can be inferred that the WSDI can also act potentially to detect groundwater drought as suggested by Abhishek (2022).

Overall, different drought indices have different limitation and their ideal performance relies on having access to different data, and effective data processing (Liu, Zhu, et al., 2022). Consequently, it seems to be unrealistic to expect a single drought index to capture all drought types and in all regions. However, the use of TWSA-based indices for drought analysis and assessment makes more sense from a physical perspective, as soil water content and total soil storage deficit are better visual representations of drought (Sun et al., 2018). The WSDI-based analysis of drought intensity suggests that the majority of the KB has undergone moderate droughts. Unfortunately, there is no similar study in the KB to be used as a validation source for the WSDI-revealed results of the current study. However, some researchers used conventional approaches and indices to assess the drought situation of

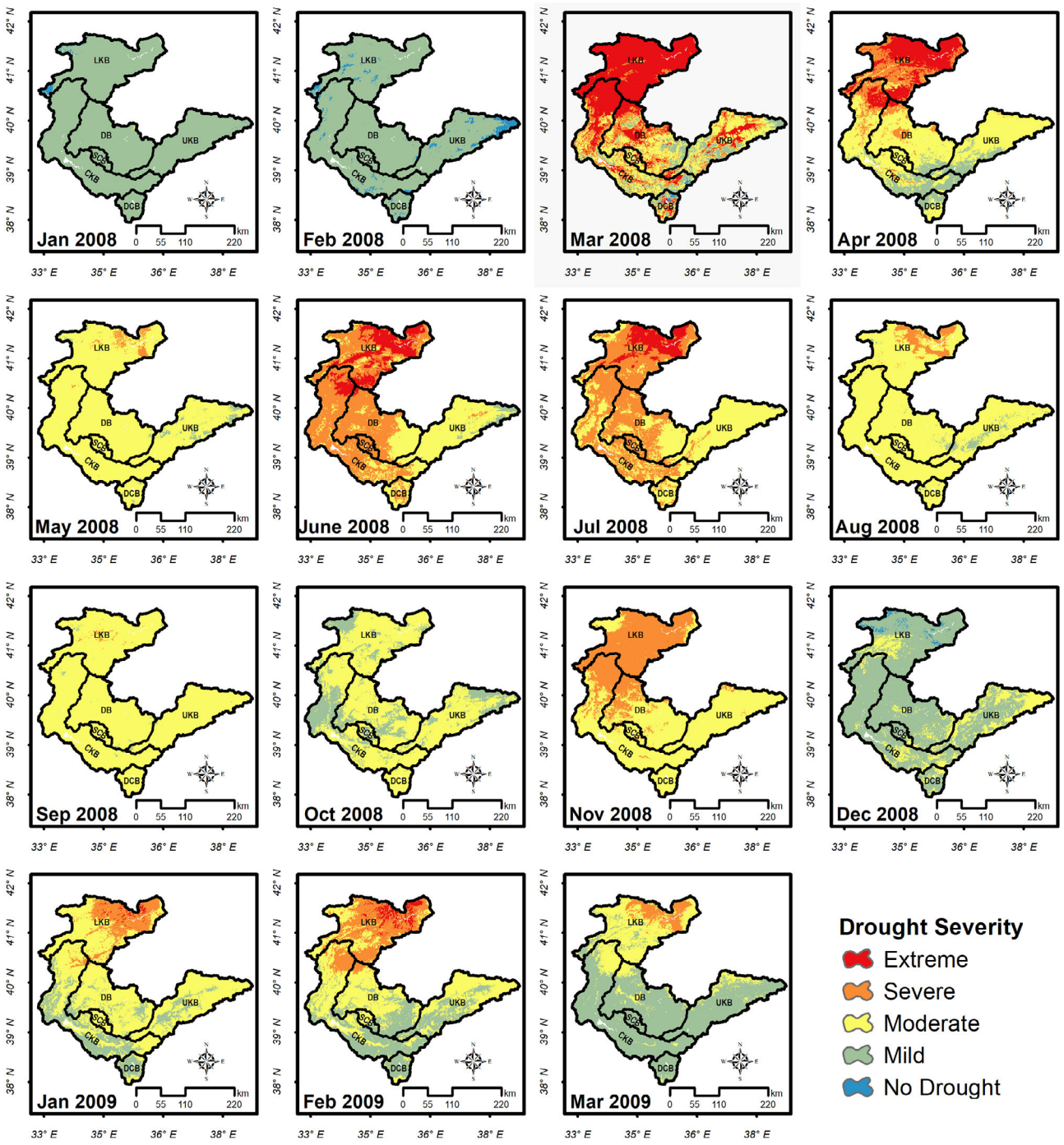

FIGURE 8 Thematic illustration of the spatial variability of the drought incident (January 2008–March 2009) based on the water storage deficit index (WSDI).

the KB. For example, taking into account the results of SPI-based analysis, Akturk et al. (2022) reported that 28 of the 31 drought-stricken stations in the KB had experienced mild droughts from 1960 to 2017. In a more recent study, Deger et al. (2023) applied Streamflow Drought Index (SDI) to analyse the dry and wet periods in the KB and found that mild droughts had the highest percentage of occurrence in the basin. These findings cast light on the feasibility of the used method for monitoring droughts at a basin scale.

4.2 | Drought conditioning parameters in the KB

Being the main feeding source of the hydrological cycle, variations in precipitation play the most important role in the onset and evolution of droughts throughout the world. The precipitation is also very effective on the fluctuations of TWSA thus affecting the water storage variations in a given area. The results of the current study revealed that there is a moderate association between the variations of

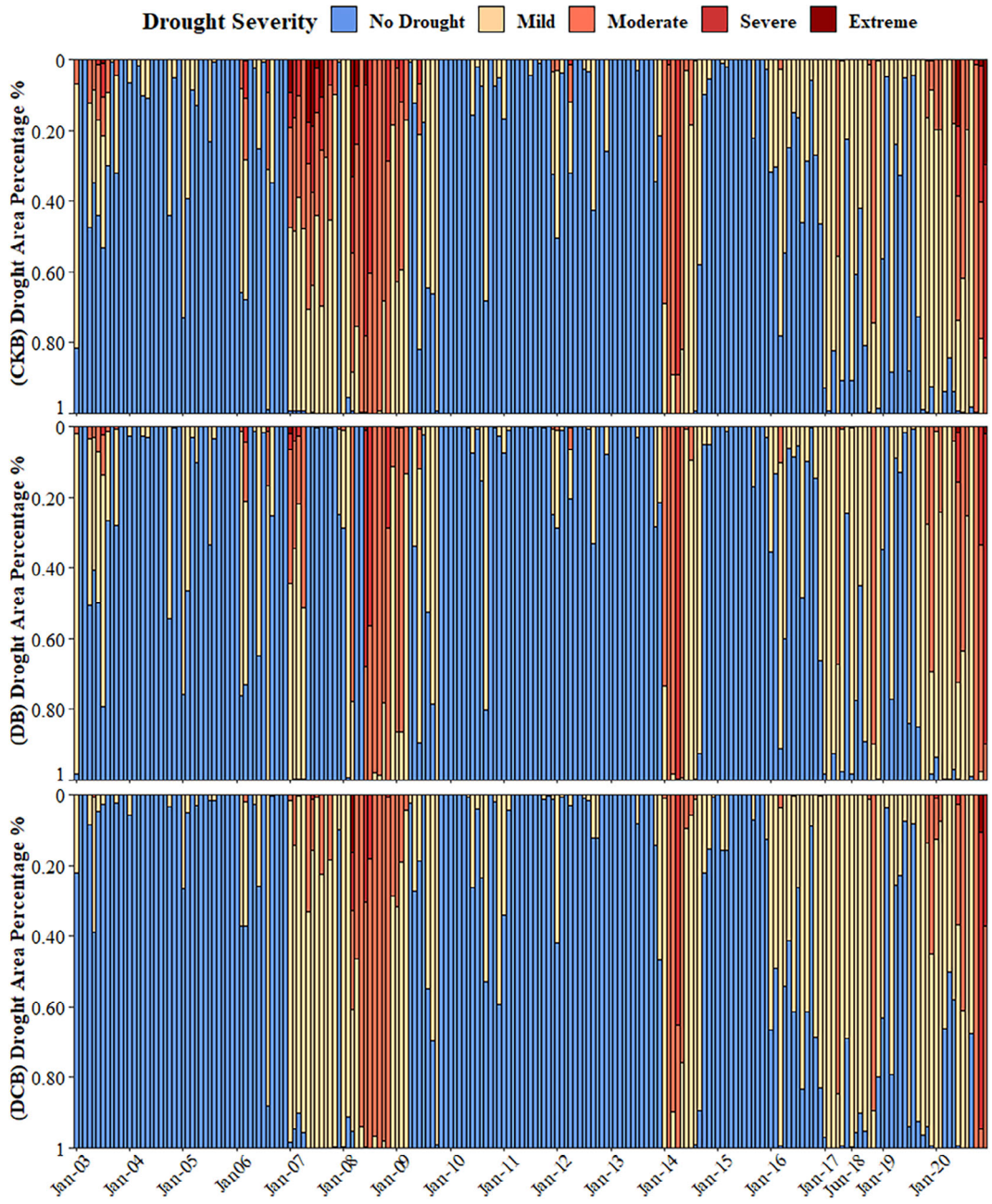

FIGURE 9 Illustration of the areal distribution of drought based on Water Storage Deficit Index (WSDI) from 2003 to 2020.

precipitation and those of TWSA. The trend analysis suggested that, notwithstanding the significance of the trends, except in the LKB, DB, SCB, and UKB subbasins, over which there is an agreement between the annual trends of precipitation and TWSA, there are contrasts over the remaining subbasins. However, the fluctuations of TWSA cannot scientifically appertain to the precipitation in the KB based on the discrepancies between the precipitation and TWSA trends in terms of statistical significance. On the other hand, because the GRACE mission considers anthropogenic forces (such as groundwater withdrawal) (Cui et al., 2021), it can be stated that the detected droughts over the KB may be mainly ascribed to anthropogenic parameters. A great part of the KB is located in central Anatolia, where water resources are crippled by the side effects of the climate crisis in an arid region (Citakoglu & Minarecioglu, 2021). Since agriculture dominates the economic activities of the residents, there is a widespread extraction of groundwater, as the only water source in the region (Bozdağ, 2016). This situation is particularly aggravated during meteorological drought periods, resulting in the detriment of its hydrologic balance and accelerating the decline of water resources (Citakoglu & Minarecioglu, 2021).

4.3 | Uncertainties

Variegated sources of uncertainty are engaged in the analysis of this study. To do away with the uncertainties associated with the GRACE

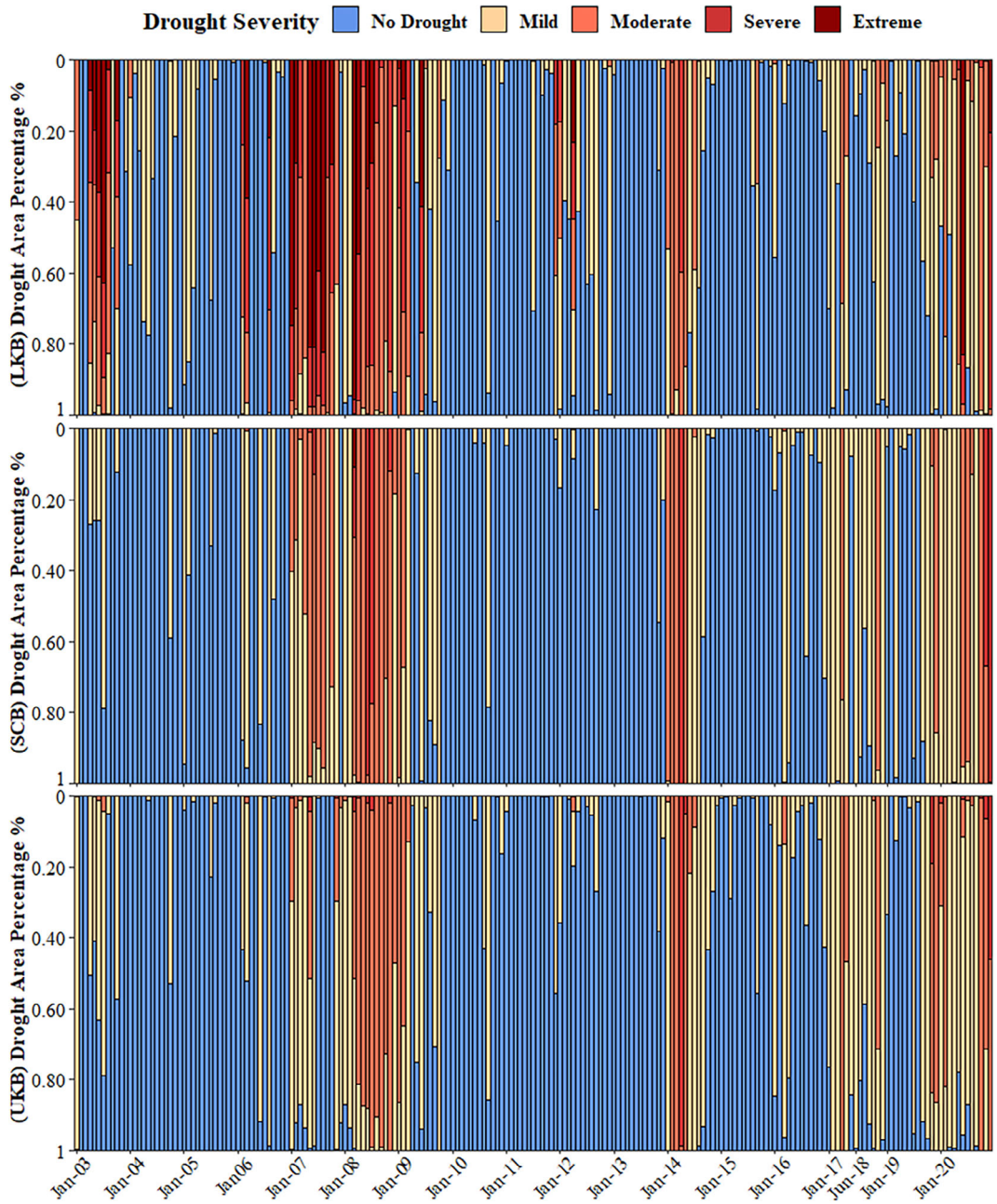

FIGURE 9 (Continued)

processing errors, the GRACE Mascon solutions were utilized for which no further processing is required and thus are deemed superior to the spherical harmonics solutions (Aryal & Zhu, 2020). However, the Mascon solutions do also suffer from some uncertainties ascribed to the applied diverse models and data processing approaches (Kumar, AnandRaj, et al., 2021). Additionally, the GRACE-derived information is subject to further uncertainties due to the errors that can be invited through the gap-filling based on the linear interpolation technique. However, since it is very straightforward to apply, linear interpolation is widely used within the scientific community (Kumar, Rathnam, & Sridhar, 2021), thus, the missed GRACE data of this study were filled in based on this method. The uncertainties of hydrological models can be dealt with by using the ensemble mean of several models (Cao et al., 2015), however, multiple models with the same spatial resolution (1 km) as the FLDAS model are not available, so the FLDAS was the only option for this study.

5 | CONCLUSIONS

The emergence of the GRACE satellite mission paved the way for effective large-scale hydrological applications and rendered assistance to scientists to better discern drought incidents, particularly in regions where insufficient data (Yirdaw et al., 2008). This study evaluates the spatiotemporal patterns of drought using a model-integrated GRACE downscaling approach. In this premise, a model-based Random Forest

TABLE 4 Summary of the area percentage of the drought events in each basin.

Drought incidents	Subbasin	Affected area (%)	
		Overall	Extreme drought
First incident Jan 2008–Mar 2009	LKB	37%	15.0%
	DB	46%	0.08%
	CKB	49%	3.0%
	DCB	53%	1.0%
	SCB	56%	0.7%
	UKB	65%	0.01%
Second incident Sep 2019–Dec 2020	LKB	52%	6.5%
	DB	62%	0.23%
	CKB	63%	3.0%
	DCB	59%	0.66%
	SCB	62%	–
	UKB	61%	–

integrated methodology is proposed to downscale the GRACE/GRACE-FO data to the fine spatial resolution of 1 km × 1 km resolution. Consequently, the fine resolution WSDI index was generated based on the downscaled TWSA from the GRACE/GRACE-FO missions and was applied alongside scPDSI, SMSP, and GWSP drought indices to analyse droughts. It has provided reliable and robust quantitative results for the variations of water storage by integrating the fine-resolution FLDAS outputs to the GRACE/GRACE-FO observations to link surface and subsurface conditions while investigating droughts. The developed methodology is the first case of the GRACE-FLDAS integrated approach for the local-scale assessment of drought. This approach can be followed in any other region in the world and hence provide a globally pertinent approach for water storage and drought analysis. The results indicated that TWSA variations exhibited various patterns in different subbasins of the study area. The LKB was the only basin with an ascending trend of TWSA, while the remaining basins showcased decreasing trends from 2003 to 2020. Notwithstanding some trivial dry events in the region, two major drought incidents over the KB were accurately determined by the proposed methodology. The first event was a 15-month length of drought between January 2008 and March 2009 and the second event was a 16-month drought period between Sep 2019 and Dec 2020.

The findings of this study cast light on the feasibility of the RF-based downscaled TWSA for analysing droughts at sub-basin scales. Nevertheless, it can be further improved by considering two distinctive points. First, the GRACE estimates are downscaled based on the statistical relationship between the input variables from hydrologic models and the target variable. The accuracy of the modelled variables plays a decisive role in the precision of the downscaled GRACE data. The global hydrological models are inevitably subject to uncertainties arising from the land surface model used, algorithms, etc. Therefore, it can be stated that even more accurate downscaled values can be obtained for other watersheds around the world if highly accurate satellite estimates of hydro-meteorological parameters are integrated into the downscaling model. The authors also hold the notion that training the downscaling models with simulations of hydro-meteorological parameters from local-scale and area-tailored models may increase the accuracy of the downscaled variable. Second, there is almost a year of data gap between GRACE and GRACE-FO missions, which shackles their effective application for consistent monitoring of droughts. Filling in the missing data in both spatial and temporal domains can be done using improved statistical techniques such that a more coherent analysis of drought can be implemented based on the GRACE estimates. However, because of the over-, and under-estimation of positive and negative TWSA values through reconstruction techniques (Bringeland & Fotopoulos, 2023), any gap-filling method needs to be implemented with enough care to avoid additional errors.

FUNDING INFORMATION

This research did not receive any specific grant from funding agencies in the public, commercial, or not-for-profit sectors.

CONFLICT OF INTEREST STATEMENT

The authors declare that they have no known competing financial interests or personal relationships that could have appeared to influence the work reported in this paper.

DATA AVAILABILITY STATEMENT

The data that support the findings of this study are available from the corresponding author upon reasonable request.

ORCID

Behnam Khorrami https://orcid.org/0000-0003-3265-372X
Shoaib Ali https://orcid.org/0000-0003-1390-0377
Orhan Gündüz https://orcid.org/0000-0001-6302-0277

REFERENCES

Abhishek, K.T. (2022). Multidecadal land water and groundwater drought evaluation in peninsular India. *Remote Sensing*, *14*(6), 1486. https://doi.org/10.3390/rs14061486

Akturk, G., Zeybekoglu, U., & Yildiz, O. (2022). Assessment of meteorological drought analysis in the Kizilirmak River basin, Turkey. *Arabian Journal of Geosciences*, *15*, 850 (2022). https://doi.org/10.1007/s12517-022-10119-0

Ali, S., Khorrami, B., Jehanzaib, M., Tariq, A., Ajmal, M., Arshad, A., Shafeeque, M., Dilawar, A., Basit, I., Zhang, L., Sadri, S., Niaz, M. A., Jamil, A., & Khan, S. N. (2023). Spatial downscaling of GRACE data based on XGBoost model for improved understanding of hydrological droughts in the Indus Basin irrigation system (IBIS). *Remote Sensing*, *15*(4), 873. https://doi.org/10.3390/rs15040873

Ali, S., Liu, D., Fu, Q., Cheema, M. J. M., Pal, S. C., Arshad, A., Pham, Q. B., & Zhang, L. (2022). Constructing high-resolution groundwater drought at spatio-temporal scale using GRACE satellite data based on machine learning in the Indus Basin. *Journal of Hydrology*, *612*(Part C), 128295. https://doi.org/10.1016/j.jhydrol.2022.128295

Ali, S., Liu, D., Fu, Q., Cheema, M. J. M., Pham, Q. B., Rahaman, M. M., Dang, T. D., & Anh, D. T. (2021). Improving the resolution of GRACE data for Spatio-temporal groundwater storage assessment. *Remote Sensing*, *13*, 3513. https://doi.org/10.3390/rs13173513

Ali, S., Wang, Q., Liu, D., Fu, Q., Rahaman, M. M., Faiz, M. A., & Cheema, M. J. M. (2022). Estimation of spatio-temporal groundwater storage variations in the lower transboundary Indus Basin using GRACE satellite. *Journal of Hydrology*, *605*, 127315. https://doi.org/10.1016/j.jhydrol.2021.127315

An, Q., He, H., Nie, Q., Cui, Y., Gao, J., Wei, C., Xie, X., & You, J. (2020). Spatial and Temporal Variations of Drought in Inner Mongolia, China. *Water (Basel)*, *12*(6), 1715. https://doi.org/10.3390/w12061715

Arshad, A., Mirchi, A., Samimi, M., & Ahmad, B. (2022). Combining downscaled-GRACE data with SWAT to improve the estimation of groundwater storage and depletion variations in the irrigated Indus basin. *Science of the Total Environment*, *838*, 156044. https://doi.org/10.1016/j.scitotenv.2022.156044

Aryal, Y., & Zhu, J. (2020). Multimodel ensemble projection of meteorological drought scenarios and connection with climate based on spectral analysis. *International Journal of Climatology*, *40*(7), 3360–3379. https://doi.org/10.1002/joc.6402

Bozdağ, A. (2016). Assessment of the hydrogeochemical characteristics of groundwater in two aquifer systems in Çumra plain, Central Anatolia. *Environmental Earth Sciences*, *75*, 674. https://doi.org/10.1007/s12665-016-5518-4

Breiman, L. (2001). Random forests. *Machine Learning*, *45*(1), 5–32.

Briffa, K. R., van der Schrier, G., & Jones, P. D. (2009). Wet and dry summers in Europe since 1750: Evidence of increasing drought. *International Journal of Climatology: A Journal of the Royal Meteorological Society*, *29*(13), 1894–1905. https://doi.org/10.1002/joc.1836

Bringeland, S., & Fotopoulos, G. (2023). Analysis of gap-filling techniques for GRACE/GRACE-FO terrestrial water storage anomalies in Canada. GRACE-FO Terrestrial Water Storage Anomalies in Canada. Available at SSRN https://ssrn.com/abstract=4471889, https://doi.org/10.2139/ssrn.4471889

Cao, Y., Nan, Z., & Cheng, G. (2015). GRACE gravity satellite observations of terrestrial water storage changes for drought characterization in the arid land of northwestern China. *Remote Sensing*, *7*(1), 1021–1047. https://doi.org/10.3390/rs70101021

Chen, H., Wanchang, Z., Ning, N., & Yuedong, G. (2019). Long-term groundwater storage variations estimated in the Songhua River Basin by using GRACE products, land surface models, and in-situ observations. *Science of the Total Environment*, *649*, 372–387. https://doi.org/10.1016/j.scitotenv.2018.08.352

Chen, J., Cazenave, A., Dahle, C., Llovel, W., Panet, I., Pfeffer, J., & Moreira, L. (2022). Applications and challenges of GRACE and GRACE follow-on satellite gravimetry. *Surveys in Geophysics*, *43*, 305–345. https://doi.org/10.1007/s10712-021-09685-x

Citakoglu, H., & Minarecioglu, N. (2021). Trend analysis and change point determination for hydro-meteorological and groundwater data of Kizilirmak basin. *Theoretical and Applied Climatology*, *145*(3), 1275–1292. https://doi.org/10.1007/s00704-021-03696-9

Cui, L., Zhang, C., Luo, Z., Wang, X., Li, Q., & Liu, L. (2021). Using the local drought data and GRACE/GRACE-FO data to characterize the drought events in mainland China from 2002 to 2020. *Applied Sciences*, *11*(20), 9594. https://doi.org/10.3390/app11209594

Deger, İ. H., Yüce, M. İ., & Musa, E. Ş. İ. T. (2023). An investigation of hydrological drought characteristics in Kızılırmak Basin, Türkiye: Impacts and trends. *Bitlis Eren Üniversitesi Fen Bilimleri Dergisi*, *12*(1), 126–139. https://doi.org/10.17798/bitlisfen.1200742

Dellal, I., & McCarl, B. A. (2010). The economic impacts of drought on agriculture: The case of Turkey. In López-Francos A (Ed.), *Economics of drought and drought preparedness in a climate change context* (pp. 169–174). CIHEAM / FAO / ICARDA / GDAR / CEIGRAM / MARM (Options Méditerranéennes: Série A. Séminaires Méditerranéens; n. 95).

DMP. (2019). Drought Management Plan of the Kizilirmak Basin. https://www.tarimorman.gov.tr/SYGM/Belgeler/S%C3%87D/K%C4%B1z%C4%B1l%C4%B1rmak%20Havzas%C4%B1%20KYP-S%C3%87D%20Kapsam%20Belirleme%20Raporu.pdf

Emerton, R. E., Stephens, E. M., Pappenberger, F., Pagano, T. C., Weerts, A. H., Wood, A. W., Salamon, P., Brown, J. D., Hjerdt, N., Donnelly, C., Baugh, C. A., & Cloke, H. L. (2016). Continental and global scale flood forecasting systems. *Wires Water*, *3*, 391–418. https://doi.org/10.1002/wat2.1137

Ercan, B., & Yüce, M. I. (2017). Trend analysis of hydro-meteorological variables of Kızılırmak Basin. *Nevsehir Journal of Science and Technology*, *6*, 333–340. https://doi.org/10.17100/nevbiltek.323640

Famiglietti, J. S. (2014). The global groundwater crisis. *Nature Climate Change*, *4*(11), 945–948. https://doi.org/10.1038/nclimate2425

FMP. (2019). Flood Management Plan of the Kizil Irmak Basin. https://mgm.gov.tr/veridegerlendirme/il-ve-ilceler-istatistik.aspx

Gerdener, H., Engels, O., Kusche, J., & Döll, P. (2020). Deriving hydrological drought indicators based on a GRACE-assimilated global hydrological model. *GU General Assembly 2020* Online, EGU2020-2577, https://doi.org/10.5194/egusphere-egu2020-2577, 2020

Guo, M., Yue, W., Wang, T., Zheng, N., & Wu, L. (2021). Assessing the use of standardized groundwater index for quantifying groundwater drought over the conterminous US. *Journal of Hydrology*, *598*, 126227. https://doi.org/10.1016/j.jhydrol.2021.126227

Gyawali, B., Murgulet, D., & Ahmed, M. (2022). Quantifying changes in groundwater storage and response to hydroclimatic extremes in a coastal aquifer using remote sensing and ground-based measurements: The Texas gulf coast aquifer. *Remote Sensing*, *14*(3), 612. https://doi.org/10.3390/rs14030612

Hinis, M. A., & Geyikli, M. S. (2023). Accuracy evaluation of standardized precipitation index (SPI) estimation under conventional assumption in Yeşilırmak, Kızılırmak, and Konya closed basins, Turkey. *Advances in Meteorology*, *2023*, 1–13. https://doi.org/10.1155/2023/5142965

Hosseini-Moghari, S. M., Araghinejad, S., Ebrahimi, K., & Tourian, M. J. (2019). Introducing modified total storage deficit index (MTSDI) for drought monitoring using GRACE observations. *Ecological Indicators*, *101*, 465–475. https://doi.org/10.1016/j.ecolind.2019.01.002

Houborg, R., Rodell, M., Li, B., Reichle, R., & Zaitchik, B. F. (2012). Drought indicators based on model-assimilated gravity recovery and climate experiment (GRACE) terrestrial water storage observations. *Water Resources Research*, *48*, W07525. https://doi.org/10.1029/2011WR011291

Hu, Z., Zhou, Q., Chen, X., Chen, D., Li, J., Guo, M., Yin, G., & Duan, Z. (2019). Groundwater depletion estimated from GRACE: A challenge of sustainable development in an arid region of Central Asia. *Remote Sensing*, *11*(16), 1908. https://doi.org/10.3390/rs11161908

Jyolsna, P. J., Kambhammettu, B. V. N. P., & Gorugantula, S. (2021). Application of random forest and multi-linear regression methods in downscaling GRACE derived groundwater storage changes. *Hydrological Sciences Journal*, *66*(5), 874–887. https://doi.org/10.1080/02626667.2021.1896719

Khorrami, B. (2023). Satellite-based investigation of water stress at the basin scale: An integrated analysis of downscaled GRACE estimates and remotely sensed data. *Journal of Hydroinformatics*, *25*, 1501–1512. https://doi.org/10.2166/hydro.2023.062

Khorrami, B., Ali, S., & Gunduz, O. (2023). Investigating the local-scale fluctuations of groundwater storage by using downscaled GRACE/-GRACE-FO JPL mascon product based on machine learning (ML) algorithm. *Water Resources Management*, *37*, 3439–3456. https://doi.org/10.1007/s11269-023-03509-w

Khorrami, B., Ali, S., Sahin, O. G., & Gunduz, O. (2023). Model-coupled GRACE-based analysis of hydrological dynamics of drying Lake Urmia and its basin. *Hydrological Processes*, *37*, e14893. https://doi.org/10.1002/hyp.14893

Khorrami, B., Arik, F., & Gunduz, O. (2021). Land deformation and sinkhole occurrence in response to the fluctuations of groundwater storage: An integrated assessment of GRACE gravity measurements, ICESat/ICESat-2 altimetry data, and hydrologic models. *GIScience & Remote Sensing*, *58*(8), 1518–1542. https://doi.org/10.1080/15481603.2021.2000349

Khorrami, B., Fistikoglu, O., & Gunduz, O. (2022). A systematic assessment of flooding potential in a semi-arid watershed using GRACE gravity estimates and large-scale hydrological modeling. *Geocarto International*, *1-22*, 11030–11051. https://doi.org/10.1080/10106049.2022.2045365

Khorrami, B., & Gunduz, O. (2021a). An enhanced water storage deficit index (EWSDI) for drought detection using GRACE gravity estimates. *Journal of Hydrology*, *603*, 126812. https://doi.org/10.1016/j.jhydrol.2021.126812

Khorrami, B., & Gunduz, O. (2021b). Evaluation of the temporal variations of groundwater storage and its interactions with climatic variables using GRACE data and hydrological models: A study from Turkey. *Hydrological Processes*, *35*(3), e14076. https://doi.org/10.1002/hyp.14076

Khorrami, B., & Gündüz, O. (2022). Detection and analysis of drought over Turkey with remote sensing and model-based drought indices. *Geocarto International*, *1-23*, 12171–12193. https://doi.org/10.1080/10106049.2022.2066197

Khorrami, B., & Gündüz, O. (2023). Remote sensing-based monitoring and evaluation of the basin-wise dynamics of terrestrial water and groundwater storage fluctuations. *Environmental Monitoring and Assessment*, *195*, 868. https://doi.org/10.1007/s10661-023-11480-7

Khorrami, B., Pirasteh, S., Ali, S., Sahin, O. G., & Vaheddoost, B. (2023). Statistical downscaling of GRACE TWSA estimates to a 1-km spatial resolution for a local-scale surveillance of flooding potential. *Journal of Hydrology*, *624*, 129929. https://doi.org/10.1016/j.jhydrol.2023.129929

Kisi, O., Gorgij, A. D., Zounemat-Kermani, M., Mahdavi-Meymand, A., & Kim, S. (2019). Drought forecasting using novel heuristic methods in a semi-arid environment. *Journal of Hydrology*, *578*, 124053. https://doi.org/10.1016/j.jhydrol.2019.124053

Kumar, K. S., AnandRaj, P., Sreelatha, K., Bisht, D. S., & Sridhar, V. (2021). Monthly and seasonal drought characterization using grace-based groundwater drought index and its link to teleconnections across South Indian River basins. *Climate*, *9*(4), 56. https://doi.org/10.3390/cli9040056

Kumar, K. S., Rathnam, E. V., & Sridhar, V. (2021). Tracking seasonal and monthly drought with GRACE-based terrestrial water storage assessments over major river basins in South India. *Science of the Total Environment*, *763*, 142994. https://doi.org/10.1016/j.scitotenv.2020.142994

Kurnaz, L. (2014). *Drought in Turkey*. İstanbul Policy Center.

Li, B., & Rodell, M. (2015). Evaluation of a model-based groundwater drought indicator in the conterminous US. *Journal of Hydrology*, *526*, 78–88. https://doi.org/10.1016/j.jhydrol.2014.09.027

Li, B., & Rodell, M. (2021). Groundwater drought: Environmental controls and monitoring. In *Global groundwater* (pp. 145–162). Elsevier. https://doi.org/10.1016/B978-0-12-818172-0.00011-6

Li, B., Rodell, M., Kumar, S., Beaudoing, H. K., Getirana, A., Zaitchik, B. F., de Goncalves, L. G., Cossetin, C., Bhanja, S., Mukherjee, A., Tian, S., Tangdamrongsub, N., Di Long, J. N., Lee, J., Policelli, F., Goni, I. B., Daira, D., Bila, M., de Lannoy, G., … Bettadpur, S. (2019). Global GRACE data assimilation for groundwater and drought monitoring: Advances and challenges. *Water Resources Research*, *55*(9), 7564–7586. https://doi.org/10.1029/2018WR024618

Liu, J., Zhu, G., Zhao, K., Jiao, Y., Liu, Y., Yang, M., Zhang, W., Qiu, D., Lin, X., & Ye, L. (2022). GRACE combined with WSD to assess the change in drought severity in arid Asia. *Remote Sensing*, *14*(14), 3454. https://doi.org/10.3390/rs14143454

Liu, M., Pei, H., & Shen, Y. (2022). Evaluating dynamics of GRACE groundwater and its drought potential in Taihang Mountain region, China. *Journal of Hydrology*, *612*, 128156. https://doi.org/10.1016/j.jhydrol.2022.128156

Loeser, C., Rui, H., Teng, W. L., Ostrenga, D. M., Wei, J. C., Mcnally, A. L., Jacob, J., Peters-Lidard, C., & Meyer, D. J. (2020). Famine early warning systems network (FEWS NET) land data assimilation system (LDAS) and other assimilated hydrological data at NASA GES DISC. In *American Meteorological Society Annual Meeting* (No. GSFC-E-DAA-TN77212).

Longuevergne, L., Wilson, C. R., Scanlon, B. R., & Crétaux, J. F. (2013). GRACE water storage estimates for the Middle East and other regions with significant reservoir and lake storage. *Hydrology and Earth System Sciences Discussions*, *9*, 11131–11159. https://doi.org/10.5194/hessd-9-11131-2012

Mckee, T. B., Doesken, N. J., & Kleist, J. (1993). The relationship of drought frequency and duration to time scales. *American Meteorological Society*, *58*, 174–184.

McNally, A., Arsenault, K., Kumar, S., Shukla, S., Peterson, P., Wang, S., Funk, C., Peters-Lidard, C. D., & Verdin, J. P. (2017). A land data assimilation system for sub-Saharan Africa food and water security applications. *Scientific Data*, *4*, 170012. https://doi.org/10.1038/sdata.2017.12

Nigatu, Z. M., Fan, D., You, W., & Melesse, A. M. (2021). Hydroclimatic extremes evaluation using GRACE/GRACE-FO and multidecadal climatic variables over the Nile River basin. *Remote Sensing*, *13*(4), 651. https://doi.org/10.3390/rs13040651

Nischitha, V., Ahmed, S. A., Varikoden, H., & Revadekar, J. V. (2014). The impact of seasonal rainfall variability on NDVI in the Tunga and Bhadra river basins, Karnataka, India. *International Journal of Remote Sensing*, *35*(23), 8025–8043. https://doi.org/10.1080/01431161.2014.979301

Noorisameleh, Z., Gough, W. A., & Mirza, M. M. Q. (2021). Persistence and spatial–temporal variability of drought severity in Iran. *Environmental Science and Pollution Research*, *28*, 48808–48822. https://doi.org/10.1007/s11356-021-14100-4

Okay Ahi, G., & Jin, S. (2019). Hydrologic mass changes and their implications in Mediterranean-climate Turkey from GRACE measurements. *Remote Sensing*, *11*(2), 120. https://doi.org/10.3390/rs11020120

Paca, V. H. D. M., Espinoza-Dávalos, G. E., Moreira, D. M., & Comair, G. (2020). Variability of trends in precipitation across the Amazon River basin determined from the CHIRPS precipitation product and from station records. *Water*, *12*(5), 1244. https://doi.org/10.3390/w12051244

Palmer, W. C. (1965). *Meteorological drought* (Vol. 30). Weather Bureau US Department of Commerce.

Pekpostalci, D. S., Tur, R., Danandeh Mehr, A., Vazifekhah Ghaffari, M. A., Dąbrowska, D., & Nourani, V. (2023). Drought monitoring and forecasting across Turkey: A contemporary review. *Sustainability*, *15*(7), 6080. https://doi.org/10.3390/su15076080

Rahaman, M. M., Thakur, B., Kalra, A., Li, R., & Maheshwari, P. (2019). Estimating high-resolution groundwater storage from GRACE: A random forest approach. *Environments*, *6*(6), 63. https://doi.org/10.3390/environments6060063

Richey, A. S., Thomas, B. F., Lo, M. H., Reager, J. T., Famiglietti, J. S., Voss, K., Swenson, S., & Rodell, M. (2015). Quantifying renewable groundwater stress with GRACE. *Water Resources Research*, *51*(7), 5217–5238. https://doi.org/10.1002/2015WR017349

Rui, H., Vollmer, B., Teng, B., Loeser, C., Beaudoing, H., & Rodell, M. (2018). GRACE-assimilated drought indicators for the US drought monitor. In *American Meteorological Society (AMS) Annual Meeting* (No. GSFC-E-DAA-TN51319).

Santos, J. F., Pulido-Calvo, I., & Portela, M. M. (2010). Spatial and temporal variability of droughts in Portugal. *Water Resources Research*, *46*(3), W03503. https://doi.org/10.1029/2009WR008071

Save, H., Bettadpur, S., & Tapley, B. D. (2016). High-resolution CSR GRACE RL05 mascons. *Journal of Geophysical Research: Solid Earth*, *121*(10), 7547–7569. https://doi.org/10.1002/2016JB013007

Scanlon, B. R., Zhang, Z., Save, H., Wiese, D. N., Landerer, F. W., Long, D., Longuevergne, L., & Chen, J. (2016). Global evaluation of new GRACE mascon products for hydrologic applications. *Water Resources Research*, *52*(12), 9412–9429. https://doi.org/10.1002/2016WR019494

Sehgal, V., Sridhar, V., & Tyagi, A. (2017). Stratified drought analysis using a stochastic ensemble of simulated and in-situ soil moisture observations. *Journal of Hydrology*, *545*, 226–250. https://doi.org/10.1016/j.jhydrol.2016.12.033

Seo, J. Y., & Lee, S. I. (2019). Spatio-temporal groundwater drought monitoring using multi-satellite data based on an artificial neural network. *Water*, *11*(9), 1953. https://doi.org/10.3390/w11091953

Sinha, D., Syed, T. H., Famiglietti, J. S., Reager, J. T., & Thomas, R. C. (2017). Characterizing drought in India using GRACE observations of terrestrial water storage deficit. *Journal of Hydrometeorology*, *18*, 381–396. https://doi.org/10.1175/JHM-D-16-0047.1

Sinha, D., Syed, T. H., & Reager, J. T. (2019). Utilizing combined deviations of precipitation and GRACE-based terrestrial water storage as a metric for drought characterization: A case study over major Indian river basins. *Journal of Hydrology*, *572*, 294–307. https://doi.org/10.1016/j.jhydrol.2019.02.053

Sun, Z., Zhu, X., Pan, Y., Zhang, J., & Liu, X. (2018). Drought evaluation using the GRACE terrestrial water storage deficit over the Yangtze River basin, China. *Science of the Total Environment*, *634*, 727–738. https://doi.org/10.1016/j.scitotenv.2018.03.292

Tapley, B. D., Bettadpur, S., Ries, J. C., Thompson, P. F., & Watkins, M. M. (2004). GRACE measurements of mass variability in the earth system. *Science*, *305*(5683), 503–505. https://doi.org/10.1126/science.1099192

Tariq, A., Ali, S., Basit, I., Jamil, A., Farmonov, N., Khorrami, B., Khan, M. M., Sadri, S., Baloch, M. Y. J., Islam, F., Junaid, M. B., & Hatamleh, W. A. (2023). Terrestrial and groundwater storage characteristics and their quantification in the Chitral (Pakistan) and Kabul (Afghanistan) river basins using GRACE/GRACE-FO satellite data. *Groundwater for Sustainable Development*, *23*, 100990. https://doi.org/10.1016/j.gsd.2023.100990

Thomas, A. C., Reager, J. T., Famiglietti, J. S., & Rodell, M. (2014). A GRACE-based water storage deficit approach for hydrological drought characterization. *Geophysical Research Letters*, *41*, 1537–1545. https://doi.org/10.1002/2014GL059323

Trenberth, K. E., Dai, A., Van Der Schrier, G., Jones, P. D., Barichivich, J., Briffa, K. R., & Sheffield, J. (2014). Global warming and changes in drought. *Nature Climate Change*, *4*, 17–22. https://doi.org/10.1038/nclimate2067

Komuscu, A. U. (1999). Using the SPI to analyze spatial and temporal patterns of drought in Turkey. *Drought Network News (1994-2001)*, 49.

Van der Schrier, G., Jones, P. D., & Briffa, K. R. (2011). The sensitivity of the PDSI to the Thornthwaite and penman-monteith parameterizations for potential evapotranspiration. *Journal of Geophysical Research: Atmospheres*, *116*(D3), D03106. https://doi.org/10.1029/2010JD015001

Vicente-Serrano, S., Beguería, M. S., & López-Moreno, J. I. (2010). A multiscalar drought index sensitive to global warming: The standardized precipitation evapotranspiration index. *Journal of Climate*, *23*, 1696–1718. https://doi.org/10.1175/2009JCLI2909.1

Wang, H., Xiang, L., Steffen, H., Wu, P., Jiang, L., Shen, Q., Li, Z., & Hayashi, M. (2022). GRACE-based estimates of groundwater variations over North America from 2002 to 2017. *Geodesy and Geodynamics*, *13*(1), 11–23. https://doi.org/10.1016/j.geog.2021.10.003

Wang, J., Chen, Y., Wang, Z., & Shang, P. (2020). Drought evaluation over Yangtze River basin based on weighted water storage deficit. *Journal of Hydrology*, *591*, 125283. https://doi.org/10.1016/j.jhydrol.2020.125283

Wang, P., & Pozdniakov, S. P. (2014). A statistical approach to estimating evapotranspiration from diurnal groundwater level fluctuations. *Water Resources Research*, *50*(3), 2276–2292. https://doi.org/10.1002/2013WR014251

Wang, Q., Yang, Y., Liu, Y., Tong, L., Zhang, Q. P., & Li, J. (2019). Assessing the impacts of drought on grassland net primary production at the global scale. *Scientific Reports*, *9*, 14041. https://doi.org/10.1038/s41598-019-50584-4

Wells, N., Goddard, S., & Hayes, M. J. (2004). A self-calibrating Palmer drought severity index. *Journal of Climate*, *17*(12), 2335–2351. https://doi.org/10.1175/1520-0442(2004)017<2335:ASPDSI>2.0.CO;2

Xu, H. J., Wang, X. P., Zhao, C. Y., Shan, S. Y., & Guo, J. (2021). Seasonal and aridity influences on the relationships between drought indices and hydrological variables over China. *Weather and Climate Extremes*, *34*, 100393. https://doi.org/10.1016/j.wace.2021.100393

Xu, K., Yang, D., Yang, H., Li, Z., Qin, Y., & Shen, Y. (2015). Spatio-temporal variation of drought in China during 1961–2012: A climatic perspective. *Journal of Hydrology*, *526*, 253–264. https://doi.org/10.1016/j.jhydrol.2014.09.047

Yi, H., & Wen, L. (2016). Satellite gravity measurement monitoring terrestrial water storage change and drought in the continental United States. *Scientific Reports*, *6*(1), 19909. https://doi.org/10.1038/srep19909

Yin, W., Zhang, G., Liu, F., Zhang, D., Zhang, X., & Chen, S. (2022). Improving the spatial resolution of GRACE-based groundwater storage estimates using a machine learning algorithm and hydrological model. *Hydrogeology Journal*, *30*(3), 947–963. https://doi.org/10.1007/s10040-021-02447-4

Yirdaw, S. Z., Snelgrove, K. R., & Agboma, C. O. (2008). GRACE satellite observations of terrestrial moisture changes for drought characterization in the Canadian prairie. *Journal of Hydrology*, *356*(1–2), 84–92. https://doi.org/10.1016/j.jhydrol.2008.04.004

Zaitchik, B. F., Rodell, M., & Reichle, R. H. (2008). Assimilation of GRACE terrestrial water storage data into a land surface model: Results for the Mississippi river basin. *Journal of Hydrometeorology*, *9*, 535–548. https://doi.org/10.1175/2007JHM951.1

Zhang, J., Liu, K., & Wang, M. (2021). Downscaling groundwater storage data in China to a 1-km resolution using machine learning methods. *Remote Sensing*, *13*(3), 523. https://doi.org/10.3390/rs13030523

Zhao, A., Xiang, K., Zhang, A., & Zhang, X. (2022). Spatial-temporal evolution of meteorological and groundwater droughts and their relationship in the North China plain. *Journal of Hydrology*, *610*, 127903. https://doi.org/10.1016/j.jhydrol.2022.127903

Zhao, M., Geruo, A., Velicogna, I., & Kimball, J. S. (2017). A global gridded dataset of GRACE drought severity index for 2002–14: Comparison with PDSI and SPEI and a case study of the Australia millennium drought. *Journal of Hydrometeorology*, *18*(8), 2117–2129. https://doi.org/10.1175/JHM-D-16-0182.1

Zhao, M., Velicogna, I., & Kimball, J. S. (2017). Satellite observations of regional drought severity in the continental United States using GRACE-based terrestrial water storage changes. *Journal of Climate*, *30*(16), 6297–6308. https://doi.org/10.1175/JCLI-D-16-0458

Zhou, K., Wang, Y., Chang, J., Zhou, S., & Guo, A. (2021). Spatial and temporal evolution of drought characteristics across the Yellow River basin. *Ecological Indicators*, *131*, 108207. https://doi.org/10.1016/j.ecolind.2021.108207

SUPPORTING INFORMATION

Additional supporting information can be found online in the Supporting Information section at the end of this article.

How to cite this article: Khorrami, B., Ali, S., & Gündüz, O. (2023). An appraisal of the local-scale spatio-temporal variations of drought based on the integrated GRACE/GRACE-FO observations and fine-resolution FLDAS model. *Hydrological Processes*, *37*(11), e15034. https://doi.org/10.1002/hyp.15034